Effects of the Variation of Fundamental Constants in Atoms

Elizabeth J. Angstmann

A thesis submitted in satisfaction of
the requirements for the degree of
Doctor of Philosophy
in the Faculty of Science.

January 2007

THE UNIVERSITY OF
NEW SOUTH WALES

SYDNEY · AUSTRALIA

Statement of Originality

I hereby declare that this submission is my own work and to the best of my knowledge it contains no materials previously published or written by another person, or substantial proportions of material which have been accepted for the award of any other degree or diploma at UNSW or any other educational institution, except where due acknowledgement is made in the thesis. Any contribution made to the research by others, with whom I have worked at UNSW or elsewhere, is explicitly acknowledged in the thesis. I also declare that the intellectual content of this thesis is the product of my own work, except to the extent that assistance from others in the project's design and conception or in style, presentation and linguistic expression is acknowledged.

(Signed) .....

Copyright Statement

(Signed).....

(Date).....

Authenticity Statement

(Signed).....

(Date).....

Abstract

Interest in the variation of fundamental constants has recently been stimulated by claims that the fine structure constant, α, was smaller in the past. Physicists are investigating whether α is currently varying using a number of methods including atomic clock experiments and quasar absorption spectra. To date atomic clock experiments have not reached the same level of precision as the quasar results but the precision to which transition frequencies are being measured is increasing dramatically and very soon atomic clock experiments based on Earth will be able to rival or surpass the quasar results. In order to relate the change in transition frequencies to a variation of α accurate calculations of relativistic effects in atoms and their dependence upon α are needed. Other effects, such as the small shift of transition frequencies due to blackbody radiation also need to be accounted for.

In this thesis we perform accurate calculations of the dependence of transition frequencies in two-valence-electron atoms and ions on a variation of α. The relativistic Hartree-Fock method is used with many-body perturbation theory and configuration interaction methods to calculate transition frequencies.

We also consider transitions with an enhanced sensitivity to α variation. In particular, narrow lines that correspond to atomic transitions between close lying, long-lived atomic states of different configurations. The small transition frequency, coupled with differences in the electron structure ensures a strong enhancement of the relative frequency change compared to a possible change in α.

We also show that using the modified form of the Dirac Hamiltonian, as suggested by Bekenstein, does not affect the analysis of the quasar data pertaining to a measurement of α variation, nor does it affect atomic clock experiments.

Finally we have performed calculations of the size of the frequency shift induced by a static electric field on the clock transition frequencies of the hyperfine splitting in Yb^+, Rb, Cs, Ba^+, and Hg^+. The calculations are used to find the frequency shifts due to blackbody radiation which are needed for accurate frequency measurements and improvements of the limits on variation of α. Our result for Cs $[\delta\nu/E^2 = -2.26(2) \times 10^{-10}\text{Hz}/(\text{V/m})^2]$ is in good agreement with early measurements and *ab initio* calculations. We present arguments against recent claims that the actual value might be smaller. The difference ($\sim 10\%$) is

due to the continuum spectrum in the sum over intermediate states.

Contents

List of Tables

List of Figures

Acknowledgements

Firstly I would like to thank my supervisor, Victor Flambaum, for all his help and guidance. I would also like to thank my co-supervisor Vladimir Dzuba for his patience, support and explanations. Without their help this thesis could never have been written. I would also like to acknowledge the use of their computer codes that have been years in the making and everyone who has had a hand in creating and maintaining them. I would like to acknowledge Savely Karshenboim and Sasha Nevsky for their help with part of the work in this thesis.

Thanks to Julian for the thesis template, some help with programming and some very useful discussions. Thanks also to Jacinda for useful discussions along the way.

Without the support of my husband, Chris, it would have been much harder to get the thesis completed, thanks for all the proof reading and your patience. Thanks also to the rest of my family, Mum, Dad, and my sisters for helping me get through the hard parts and for some help editing at the end, thanks to my cats for not deleting too much of the thesis when they walk all over the keyboard and my dogs for the hugs.

Preface

This thesis will investigate the theory behind using atomic clocks to measure a variation of the fine structure constant, α.

The introduction will give an overview of the current limits on the variation of some of the fundamental constants. It will give a very brief background into some of the theories about how and why fundamental constants may vary. Current limits on the variation of α will be given and there will be some discussion of how atomic clock experiments aiming to measure α variation work.

Chapters 2, 3, 4 and 5 will present my work which involves calculations to assist in a measurement of limits on α variation in the laboratory. Chapter 2 will describe how the energy levels in an atom move if α is varying and how we calculate these values. In Chapter 3 various ways to increase the sensitivity of atomic clock experiments to a variation of α will be considered. Chapter 4 puts to rest a concern raised about whether the method used to measure α variation using quasar spectra and atomic clocks is correct. In Chapter 5 we consider the effect of blackbody radiation on the transition frequencies in atoms. This is important because this effect can have a similar order of magnitude to the a variation of α and so needs to be accounted for (it also needs to be known accurately for the definition of the second).

The work in these Chapters 2-5 is based on the following papers published in peer-reviewed journals:

E. J. Angstmann, V. A. Dzuba, and V. V. Flambaum, *Relativistic effects in two valence-electron atoms and ions and the search for variation of the fine-structure constant*, Physical Review A **70**, 014102 (2004) [1]

E. J. Angstmann, V. V. Flambaum, and S. G. Karshenboim, *Cosmological variation of the fine-structure constant versus a new interaction*, Physical Review A **70**, 044104 (2004) [2]

E. J. Angstmann, V. A. Dzuba, V. V. Flambaum, A. Yu Nevsky, and S. G. Karshenboim, *Narrow atomic transitions with enhanced sensitivity to variation of the fine structure constant*, Journal of Physics B: Atomic, Molecular and Optical Physics **39**, 1937-1944 (2006) [3]

E. J. Angstmann, V. A. Dzuba, and V. V. Flambaum, *Frequency Shift of the*

Cesium Clock Transition due to Blackbody Radiation, Physical Review Letters **97**, 040802 (2006) [4]

E. J. Angstmann, V. A. Dzuba, and V. V. Flambaum, *Frequency shift of hyperfine transitions due to blackbody radiation*, Physical Review A **74**, 023405 (2006) [5]

The following paper, which I worked on during my PhD candidature has been left out of the thesis since it deals with parity nonconservation effects (specifically the possibility of measuring nuclear anapole moments in atomic Zeeman transitions, which have variable transition frequencies) while this thesis concentrates on measuring variation of α:

E. J. Angstmann, T. H. Dinh, and V. V. Flambaum, *Parity nonconservation in atomic Zeeman transititions*, Physical Review A **72**, 052108 (2005) [6]

This thesis retains the use of first person plural, however, I made a significant contribution to all of the work presented.

Chapter 1

Introduction

1.1 Theories and Varying Constants

All metric theories of gravity, such as general relativity, forbid the temporal and spatial variation of non-gravitational constants. This is because these theories are based on Einstein's equivalence principle which states that in any inertial reference frame the result of any non-gravitational experiment must be independent of where in space and when in time it is carried out. So far Einstein's equivalence principle has withstood all the tests thrown at it, however, recent measurements of a possible variation of the fine structure constant, α, (to be discussed later in the chapter) are the first indications that this theory may only be a good approximation.

The standard model of particle physics makes no allowances for the variation of any fundamental constants, for example constants such as α, or the electron-to-proton mass ratio, m_e/m_p. The standard model has thus far withstood every test that it has been put through.

Several theories including Kaluza-Klein theories and string theories, that combine gravitational and quantum effects, allow or even require variation of funda-

mental constants. These theories are higher-dimensional theories, our four dimensional constants depend upon the value of some scalar fields and on the structure and sizes of the extra dimensions. Any evolution of the size of the higher dimensions with time could lead to a spacetime variation of our four dimensional constants. An excellent review by Uzan [7] describes the theories that predict spacetime variation of constants as well as current limits on variation of these constants. Investigating the temporal and spatial variation of constants serves as a way to probe the underlying fundamental physics and can suggest the form that a unified theory should take. Confirmation of α variation would be exciting since it would indicate new physics beyond the standard model and general relativity.

1.2 Constants that we try to constrain

To get a clearer understanding of how the universe works it is important to investigate how several of the fundamental constants are varying (or not varying!). To obtain a clear picture of the form of the true description of the universe we need to find the constraints on as many of the parameters as possible. It is important that the constants that we constrain (such as α or m_e/m_p) are dimensionless, otherwise a measurement of their variation could in fact be due to a variation of the system of units used, rather than the constant.

This thesis will concentrate on placing limits on possible variation of $\alpha(= e^2/\hbar c)$. α characterizes the strength of the electromagnetic interaction: it represents the strength of the interaction between electrons and photons. In atomic units ($m_e = 1$, $\hbar = 1$ and $e = 1$), which will be used throughout this thesis, $\alpha = 1/c$. As its name suggests the fine structure constant plays an important role in determining the fine structure of atomic energy levels. That is, it is very important for determining the size of relativistic effects in atoms. As will become clear throughout the thesis we exploit this dependence to obtain limits on its

possible variation.

Theories that predict a varying α usually predict that other constants, such as the QCD scale parameter, Λ_{QCD}, also vary. In fact, many grand unification models predict that Λ_{QCD} should vary faster than α. For example, Langacker *et al.* [8] use a typical model (a grand unified gauge theory with a single coupling constant) to predict that

$$\frac{\Delta\Lambda_{QCD}}{\Lambda_{QCD}} \sim 34\frac{\Delta\alpha}{\alpha}$$

(Calmet and Fritzsch, [9], performed a similar analysis at the same time, and obtained the coefficient 38 ± 6, which is in good agreement with Langacker *et al.*, who claim a 20% uncertainty). Neutron and proton masses are largely fixed by Λ_{QCD}. In this same model quark and electron masses scale as $\Delta m/m \sim 70\Delta\alpha/\alpha$. It is thus easy to show that for this model

$$\frac{\Delta(m_q/\Lambda_{QCD})}{(m_q/\Lambda_{QCD})} \sim 36\frac{\Delta\alpha}{\alpha}$$

where m_q/Λ_{QCD} is dimensionless. While α can be determined from the relativistic effects in atoms, m_q/Λ_{QCD} is involved in determining the size of nuclear effects and so variation of this parameter is constrained by observations of phenomena such as nuclear binding energies, resonances, nuclear magnetic moments and molecular rotational transitions (see for example [10–12]). This thesis is concerned with constraining α but a measurement of α variation would imply that many of the "constants" may not actually be constant.

1.3 Current limits on α variation

Recently there has been some very exciting evidence from quasar spectra that α may have been smaller in the past [13]. Limits can be placed on the amount of variation in α over several different timescales. Obtaining limits on different timescales is a useful exercise because it indicates to us the manner in which α

varies. For example, did it vary relatively rapidly at some time in the past and is now nearly constant, or is it continually varying at a constant rate? Of course there are an infinite number of options for the functional form but by increasing the number of data points we can get a much better idea of the function. Each different timescale has its own advantages and disadvantages. Assuming that the rate of change of α is always in the same direction (i.e. getting bigger or smaller) then the further back in time we look the less precision we need to make our detection. Of course if you lose the fixed sign of the rate of change of α then looking back over long timescales can potentially give a null result when variation is present and definitely will underestimate the amount of variation. This means that this method could completely miss any oscillatory variation of α. Also looking back a long time into the past can obviously only tell us of past α variation and not about the present behavior of α.

A number of theories have been suggested to describe the variation of α throughout the history of the universe. Sandvik *et al.* [14] suggest a theory in which α remains almost constant during the radiation era, then increases slightly during the matter era but then once again approaches a constant value when the expansion of the universe starts to accelerate. To distinguish between theories and to ascertain whether theories such as this one are feasible it is important to probe α variation on a number of different timescales. Both quasar results and laboratory experiments have an important place in determining how the universe works.

There are three main methods used to place competitive limits on the variation of α; quasar spectra, the Oklo uranium mine, and atomic clock experiments. The limits obtained to date using each of these methods are discussed below.

Table 1.1: Limits on α variation from quasar spectra.

Reference	$\Delta\alpha/\alpha$	Redshift	Technique[a]
Murphy *et al.*[15]	$(-0.574 \pm 0.102)\times10^{-5}$	$0.2 < z < 3.7$	MM
Quast *et al.* [16]	$(-0.04 \pm 0.19 \pm 0.27_{sys})\times10^{-5}$	1.15	RMM
Srianand *et al.* [17]	$(-0.06 \pm 0.06)\times10^{-5}$	$0.4 < z < 2.3$	MM

[a] MM stands for the many-multiplet technique and RMM stands for regressional many-multiplet technique described in [16].

1.3.1 Limits on α variation from quasar spectra

One method of determining whether α has varied is to analyze the absorption spectrum of dust clouds imposed on quasar emission spectra to see whether α was different in the past, when the light was absorbed by the dust clouds. The big advantage of using quasars is that they are situated at relatively large redshifts, $z \sim 0.5 - 3.5$ and so studying them allows us to peer into the ancient history of the universe. This is a large advantage because if α was varying steadily through time we would expect to see the largest change in the oldest spectral lines. Alternatively, if α varied suddenly, then since this data spans a larger percentage of the universe's history, the time at which α varied is more likely to be contained within this data. Several groups are currently working on obtaining limits on α variation from quasar spectra. There is some discrepancy among the results obtained by the different groups. The current limits on $\Delta\alpha/\alpha$ obtained in this manner are shown in the Table 1.1.

The results obtained by Murphy *et al.* [15] indicate that α was smaller in the past. This observation was based on quasars with redshifts in the range $0.2 < z < 3.7$, which corresponds to a time separation of $2.5 - 12.2$ Gyr in the currently popular model with $\Omega_\Lambda = 0.7$, $\Omega_{\text{matter}} = 0.3$, and $H_0 = 68\ \text{kms}^{-1}\text{Mpc}^{-1}$. If we assume that α varied constantly over this period (there is no reason to assume this but it is useful as an indication of the kind of accuracies that we hope atomic clock experiments will achieve to be competitive with the quasar

results), this corresponds to $\dot{\alpha}/\alpha = (-0.72 \pm 0.16) \times 10^{-15}$ per year. However no indication of α variation was found by other groups also using astrophysical observations; $\Delta\alpha/\alpha = (-0.06 \pm 0.06) \times 10^{-5}$ in the redshift range $0.4 < z < 2.3$ [17] corresponding to a constant change $\dot{\alpha}/\alpha = (-0.08 \pm 0.08) \times 10^{-15}$ per year and $\Delta\alpha/\alpha = (-0.04 \pm 0.33) \times 10^{-5}$ in the redshift range $z \simeq 1.15$ [16] which corresponds to $\dot{\alpha}/\alpha = (-0.05 \pm 0.38) \times 10^{-15}$ per year. Until very recently there was no obvious reason to consider one group's data more convincing than another. However, Murphy *et al.* [18] have recently claimed that Srianand *et al.* [17] used a flawed parameter estimation method and as a result they underestimated the size of the uncertainties and overestimated the size of α in the past. They estimate that the correct result from the data is $(-0.44 \pm 0.16) \times 10^{-5}$ bringing the result for $\Delta\alpha/\alpha$ closer to their result. It may also be the case that some other effect, such as a possible spatial variation of α, could bring all the results into agreement. The data used in [15] comes from different hemispheres than the data used in [16, 17]. It should be noted that all the groups analyze their results in the same way. The method they use, once the redshift and observational uncertainties have been accounted for, are exactly the same as the method used to analyze laboratory spectra. The calculations of the relativistic energy shifts in atoms performed by our group are used by the quasar groups to interpret their data.

1.3.2 Limits on α variation from Oklo

Another method to place limits on α variation involves the Oklo uranium mine, which is situated in Gabon in West Africa. It contained a natural fission reactor that was active 1.8×10^9 years ago. The present isotopic abundances allow the reaction rates, from when the fission reactor was active to be extracted. This in turn allows a bound on changes in α to be extracted [19–23]. The most recent limit obtained in this way is $\Delta\alpha/\alpha = 4.5^{+1.5}_{-0.7} \times 10^{-8}$ [22], where $\Delta\alpha$ is the change in α since the fission reactor was active, this corresponds to a redshift, $z \sim 0.14$.

Note that this is a positive value, indicating that α was larger in the past, the opposite of the quasar result (both results could be correct if α was varying in an oscillatory fashion). One of the problems with a limit on α variation obtained in this way is that there are a number of assumptions made in deriving the value, such as model dependent assumptions about how the variation of one constant affects the variation of another. Flambaum and Shuryak [24] argue that a more reasonable interpretation of the Oklo data is a variation of the ratio of the quark mass to the QCD scale, $\delta(m_s/\Lambda_{QCD})/(m_s/\Lambda_{QCD}) = -(0.56 \pm 0.05) \times 10^{-9}$, here m_s is the mass of the strange quark, since a change in the resonance energy is much (170 times) more sensitive to a change in this parameter than to a change in α.

1.3.3 Limits on α variation from laboratory clocks

Atomic clock experiments have several advantages over other methods of measuring possible α variation. Firstly, they are more reliable and reproducible than other ways of measuring α variation since better statistics can be produced and it is easier to control systematics. This is impossible, for example, with quasars, only the systematics coming into making the measurements can be controlled, you can not set up the quasar to produce the ideal results by, for example, choosing the atomic abundances. Secondly, atomic clocks are extremely sensitive. Great leaps forward have been made with the introduction of the frequency comb. Measurements of frequency changes have been made to an accuracy of the order of 10^{-15} in Rb [25], Yb^+ [26, 27], and Hg^+ [28, 29] and this year a measurement of the Hg^+ ion ultraviolet transition frequency was measured with respect to the cesium standard with a fractional uncertainty of only 9.1×10^{-16} [30]. Thirdly, atomic clock experiments are sensitive to an oscillatory variation of α. While quasars can be used to probe the value of α billions of years ago and compare it to its current value they could overlook any change over a smaller timescale. In

contrast atomic clock experiments are able pick up these changes. Atomic clock experiments look for changes in α over a period of months to a few years. Atomic clock experiments only probe temporal variations of α, not spatial ones since they are all conducted on the Earth. This makes the results slightly easier to interpret than the quasar results that could indicate a temporal or a spatial variation of α.

Laboratory experiments work by comparing the frequency of two atomic clocks at two different times. The atomic clocks need to be carefully selected so that the change in frequencies can be related to a change in α. Optical atomic clock transitions are suitable because the ratio of the frequencies of the optical transitions depend on α alone. This is because they are either gross structure transitions (transitions between levels with different n or n^*) or transitions between levels with a different fine structure (same n but a different j). In these cases we can obtain a limit on α variation because the dependence of the frequency on α is well understood. Hyperfine transition frequencies depend upon α but also upon the nuclear magnetic moment and m_e/m_p, and so it is harder to interpret the results of a frequency shift since it is unclear how much of the frequency shift is a result of a change in m_e/m_p or the nuclear magnetic moment (or the proton gyromagnetic ration, g_p that helps to determine the magnetic moment) and how much of the frequency shift is due to a variation of α. This is discussed in the review by Karshenboim [31].

Several atomic clock type experiments have placed limits on present day α variation. These experiments do not yet match the precision of the quasar limits, though they are getting very close; they are presented in Table 1.2. Note that the limit obtained from the hyperfine transition Marion *et al.* [25] is obtained by assuming that all of the time variation is due to a variation of α, which as they point out is unlikely to be the case. In fact, this is a problem for all but the first four results in the Table 1.2. These more recent results were obtained using multiple transitions to separate the α dependance from the dependance

Table 1.2: Limits on α variation from atomic clock experiments.

Reference	$\dot{\alpha}/\alpha$ per year	First Atomic Clock	Reference Atomic Clock
Peik *et al.* [27]	$(-0.26\pm0.39)\times10^{-15}$	$^{171}Yb^{+}$	$^{199}Hg^{+}$[a]
Cingöz *et al.* [37]	$(-2.7 \pm 2.6) \times 10^{-15}$	^{163}Dy	^{162}Dy [b]
Peik *et al.* [26]	$(-0.3 \pm 2.0) \times 10^{-15}$	$^{171}Yb^{+}$	$^{199}Hg^{+}$[c]
Fischer *et al.* [38]	$(-0.9 \pm 2.9) \times 10^{-15}$	H	$^{199}Hg^{+}$[d]
Bize *et al.* [29]	$\lvert\dot{\alpha}/\alpha\rvert < 1.2 \times 10^{-15}$	$^{199}Hg^{+}$	^{133}Cs
Marion *et al.* [25]	$-0.4 \pm 16 \times 10^{-16}$	^{87}Rb	^{133}Cs
Prestage *et al.* [39]	$\leq 3.7 \times 10^{-14}$	Hg^{+}	H-maser
Godone *et al.* [40]	$\leq 2.7 \times 10^{-13}$	^{24}Mg	^{133}Cs

[a] Peik *et al.* used data from [26, 29] along with the new measurement of the Hg^{+} transition frequency with respect to Cs obtained by Oskay *et al.* [30] to obtain this limit on α variation.

[b] Cingöz *et al.* use nearly degenerate levels in dysprosium that are especially sensitive to a variation of α (this is discussed in Chapter 3). The dysprosium transitions are referenced to a cesium standard.

[c] Peik *et al.* actually used three transition frequencies to obtain their limit on α variation. They measured the drift of the $^{171}Yb^{+}$ frequency against the ^{133}Cs clock frequency and then used the result for $^{199}Hg^{+}$ obtained by Bize *et al.* [29] to get a limit on α variation independent of any variation of the magnetic moments.

[d] Fischer *et al.* combined their measurement of the drift of the H transition frequency with respect to the Cs transition frequency with the results obtained by Bize *et al.* [29] and Marion *et al.* [25] to get limit on α variation.

on the magnetic moments. Flambaum and Tedesco [32] calculate the relative sensitivity of the atomic transitions listed in Table 1.2 and others to a variation in α and a variation of m_q/Λ_{QCD}, where m_q is quark mass. It has been suggested by Nguyen *et al.* [33] that a sensitivity of $|\dot{\alpha}/\alpha| < 1.2 \times 10^{-18}$ per year could be reached by using the accidentally degenerate levels in Dysprosium, as suggested in [34]. There are many proposals for the search of variation of α in atomic optical transitions, such as those suggested in [34–36]. More laboratory experiments are vital in order to place even more stringent limits on present day α variation.

To date almost all laboratory experiments are compatible with no variation of α to within 1σ. The outlook for atomic clock experiments is good; the obtainable accuracy is improving with new techniques and equipment. In order to convert accurate measurements into accurate limitations on the amount of variation of

constants such as α we need accurate calculations of the effect of any variation on the transition frequencies of atomic clocks. This is the focus of this thesis, predicting how changes in the value of α will shift transition frequencies. We also suggest some transitions in which the frequencies are very sensitive to α variation which makes them good probes for variation of α.

Chapter 2

Relativistic effects in two valence electron atoms and ions

If the fine structure constant, α, is changing it will cause atomic transition frequencies to drift over time. In order to measure how large any change in α it is necessary to know how shifts in the atomic energy spectrum are related to α variation. In this chapter an explanation of how to calculate the shift in atomic transition frequencies with a change of α is given and results are presented. We have calculated the size of the frequency shift in two valence electron atoms and ions. Other members of our group have performed these calculations for other atoms. These calculations are needed to interpret both atomic clock experiments and quasar results in terms of a varying α.

The work presented in this chapter is based upon the work presented in Angstmann *et al.* published in Physical Review A [1] and the pre-print Angstmann *et al.* [41].

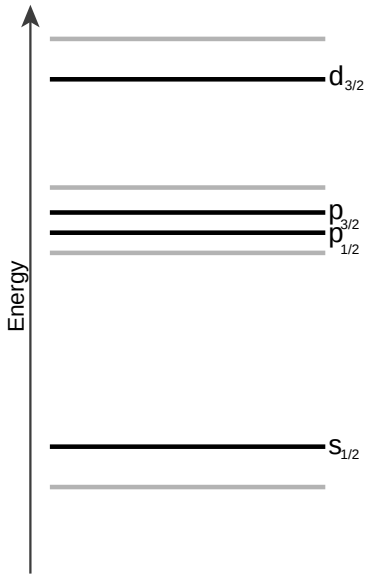

Figure 2.1: If α is increasing over time this will cause a small shift in the energy spectrum of an atom and hence in the transition frequencies. As a rule of thumb the energies of the $s_{1/2}$ and $p_{1/2}$ levels decrease as α increases and the others increase. This is shown schematically and not to scale for an unspecified atom in the figure. The black lines represent the initial energy levels and the grey lines indicate where the energy levels will move to if α increases.

2.1 Introduction

Laboratory measurements of α variation involve measuring how the difference between two atomic transition frequencies changes with time. To relate a measurement of the change between two frequencies to a change in α, the relativistic energy shifts are needed. The relativistic energy shift describes how a level moves as α varies. Two transition frequencies with very different relativistic energy shifts are the most desirable candidates for precision experiments as they will have the largest relative frequency shift between them. This effect is represented schematically in Figure 2.1.

In this chapter we perform relativistic many-body calculations to find the relativistic energy shift for many two valence electron atoms and ions. Two valence electron atoms and ions were chosen since many new optical clocks experiments,

some of which are currently under construction and some still under consideration, utilize these atoms and ions (e.g.: Al II [42], Ca I [28], Sr I [43–45], In II [46–48], Yb I, Hg I [49, 50]).

The relativistic Hartree-Fock method is used with many-body perturbation theory and configuration interaction methods to calculate transition frequencies. In the rest of the chapter we will give an outline of how we calculate the atomic energy levels and then how these calculations are changed to evaluate the effect of α variation.

2.2 Calculations of Atomic Energy Levels

Here we perform calculations for closed sub-shell atoms and ions which can also be considered as atoms/ions with two valence electrons above closed shells. We start our calculations from the relativistic Hartree-Fock (RHF) (also known as Dirac-Hartree-Fock) method in the V^N approximation. This means that RHF calculations are done for the ground state of the corresponding atom/ion with all electrons included in the self-consistent field. The use of the V^N RHF approximation ensures good convergence of the consequent configuration interaction (CI) calculations for the ground state. Good accuracy for excited states is achieved by using a large set of single-electron states. Note that there is an alternative approach which uses the V^{N-2} starting approximation (with two valence electrons removed from the RHF calculations). This approach has some advantages; it is simpler and ground and excited states are treated equally. However, the convergence with respect to the size of the basis is not as good and the final results are better in the V^N approximation. We use the V^{N-2} approximation as a test of the accuracy of calculations of the relativistic energy shifts, while presenting all final results in the V^N approximation.

We use a form of the single-electron wave function that explicitly includes a

dependence on α:

$$\psi(\mathbf{r})_{njlm} = \frac{1}{r}\begin{pmatrix} f(r)_n \Omega(\mathbf{r}/r)_{jlm} \\ i\alpha g(r)_n \tilde{\Omega}(\mathbf{r}/r)_{jlm} \end{pmatrix}. \tag{2.1}$$

This leads to the following form of the RHF equations (in atomic units):

$$\begin{aligned} f_n^{'}(r) + \frac{\kappa_n}{r} f_n(r) - [2 + \alpha^2(\epsilon_n - \hat{V}_{HF})] g_n(r) = 0, \\ g_n^{'}(r) + \frac{\kappa_n}{r} g_n(r) + (\epsilon_n - \hat{V}_{HF}) f_n(r) = 0, \end{aligned} \tag{2.2}$$

where $\kappa = (-1)^{l+j+1/2}(j + 1/2)$, n is the principle quantum number and $\hat{V}_{HF}$ is the Hartree-Fock potential. The non-relativistic limit corresponds to setting $\alpha = 0$.

We then use the combination of the configuration interaction (CI) method with many-body perturbation theory (MBPT)[51, 52]. Interactions between valence electrons are treated using the CI method while correlations between the valence electrons and the core electrons are included by means of MBPT. We can write the effective CI Hamiltonian for two valence electrons as:

$$\hat{H}^{CI} = \hat{h}_1 + \hat{h}_2 + \hat{h}_{12} \tag{2.3}$$

here $\hat{h_i}$ ($i = 1$ or 2) is an effective single-electron Hamiltonian given by

$$\hat{h_i} = c\boldsymbol{\alpha} \cdot \mathbf{p} + (\beta - 1)mc^2 - \frac{Ze^2}{r_i} + \hat{V}_{core} + \hat{\Sigma}_1, \tag{2.4}$$

$\mathbf{p}$ is the electron momentum, $\boldsymbol{\alpha}$ is the Dirac matrix, $\hat{V}_{core}$ is the Hartree-Fock potential created by the core electrons, it differs from $\hat{V}_{HF}$ in Eq. (2.2) by the contribution of the valence electrons. $\hat{\Sigma}_1$ is the one-electron operator that describes the correlation interaction between a valence electron and the core. The third term in Eq. (2.3) describes the interaction of the valence electrons with each other and can be written as

$$\hat{h}_{12} = \frac{e^2}{r_{12}} + \hat{\Sigma}_2 \tag{2.5}$$

where $\hat{\Sigma}_2$ is a two-particle operator that describes the effects of screening of the Coulomb interaction between the valence electrons by the core electrons. The operators $\hat{\Sigma}_1$ and $\hat{\Sigma}_2$ are calculated using the second order of MBPT.

We use the same set of single-electron basis states to construct two-electron wave functions for the CI calculations and to calculate the $\hat{\Sigma}$'s. The set is based on the B-spline technique developed by Johnson *et al* [53–55]. We use 40 B-splines in a cavity of radius $R = 40a_B$ (a_B is Bohr radius). The single-electron basis functions are linear combinations of 40 B-splines and are also eigenstates of the Hartree-Fock Hamiltonian (in the V^N potential). Therefore, we have 40 basis functions in each partial wave including the B-spline approximations to the atomic core states. We use a different number of basis states for the CI wave functions and for the calculations of the $\hat{\Sigma}$'s. Saturation comes much faster for the CI calculations. In these calculations we use 14 states above the core in each partial wave up to $l_{max} = 3$. Inclusion of states of higher principal quantum number or angular momentum does not change the result. To calculate the $\hat{\Sigma}$'s we use 30 out of 40 states in each partial wave up to $l_{max} = 4$.

The results for the energies are presented in Table 2.1. We present the energies of the $nsnp$ configuration of two electron atoms/ions with respect to their ground state $^1S_0$ ns^2. The states considered for atomic clock experiments are $^3P_0$ and $^3P_1$. However, we present the result for other states as well for completeness, these also make it easier to analyze the accuracy of the calculations. Also, transitions associated with some of these states are observed in quasar absorption spectra (e.g., the $^1S_0 - ^1P_1$ transition in Ca).

To demonstrate the importance of the core-valence correlations we include results of pure CI calculations (with no $\hat{\Sigma}$'s) as well as the results in which $\hat{\Sigma}_1$ is included but $\hat{\Sigma}_2$ is not. One can see that the accuracy of pure CI calculations is about 10% while inclusion of core-valence correlations improves it significantly to the level of about 1%. The deviation from experiment of the final theoretical

Table 2.1: Energies of the *nsnp* configuration of two electron atoms calculated using H^{CI}, $H^{CI}+\hat{\Sigma}_1$ and $H^{CI}+\hat{\Sigma}_1+\hat{\Sigma}_2$; comparison with experiment (cm^{-1})

Atom/ ion	State	Experiment [56]	Theory $\hat{H}^{CI}$	$\hat{H}^{CI}+\hat{\Sigma}_1$	$\hat{H}^{CI}+\hat{\Sigma}_{1,2}$
AlI	$^3P_0$	37393	36403	36987	37328
	$^3P_1$	37454	36466	37053	37393
	$^3P_2$	37578	36592	37185	37524
	$^1P_1$	59852	59794	60647	60090
CaI	$^3P_0$	15158	13701	14823	15011
	$^3P_1$	15210	13750	14881	15066
	$^3P_2$	15316	13851	14997	15179
	$^1P_1$	23652	23212	24968	24378
SrI	$^3P_0$	14318	12489	13897	14169
	$^3P_1$	14504	12661	14107	14367
	$^3P_2$	14899	13021	14545	14786
	$^1P_1$	21698	20833	23012	22305
InII	$^3P_0$	42276	37825	39238	42304
	$^3P_1$	43349	38867	40394	43383
	$^3P_2$	45827	41168	42974	45904
	$^1P_1$	63034	62181	64930	62325
YbI	$^3P_0$	17288	14377	16352	16950
	$^3P_1$	17992	15039	17189	17705
	$^3P_2$	19710	16550	19137	19553
	$^1P_1$	25068	24231	27413	26654
HgI	$^3P_0$	37645	31864	32692	37420
	$^3P_1$	39412	33751	34778	39299
	$^3P_2$	44043	38155	39781	44158
	$^1P_1$	54069	50247	52994	56219
TlII	$^3P_0$	49451	43831	43911	49865
	$^3P_1$	52393	47091	47350	52687
	$^3P_2$	61725	55988	56891	62263
	$^1P_1$	75660	74291	76049	74717

energies for the triplet states of all atoms except Yb is not more than 1%. For Yb it is 2%. The accuracy of the singlet states is about 1% for AlII, 2% for TlII, 3-4% for CaI, SrI, InII and YbI and 6% for HgI. The accuracy of the fine structure intervals ranges from 2 to 7%. The accuracy of calculations for Yb is not as good as for the other atoms because the two electron approximation is a poor approximation for this atom. Electrons from the $4f$ subshell, which are kept frozen in the present calculations, are relatively easy to excite and the corresponding configurations give a substantial contribution to the energy. Note that we do include these excitations perturbatively into the $\hat{\Sigma}$ operators. However, due to their large contribution, second-order treatment of the excitations from the $4f$ subshell is not very accurate. On the other hand, the CI+MBPT results for Yb are still much better than pure CI values. The calculations are more accurate for the triplet states than the singlet states. This is because more mixing occurs with the singlet state (due to nearby levels with the same parity) than with the triplet ones.

Note also that the CI+MBPT results presented in Table 2.1 are in good agreement with similar calculations in Refs. [57, 58].

2.3 Calculations of Transition Frequency Shifts with α Variation

Now that we have an accurate method of calculating the energy levels of the atoms and ions, which includes the explicit dependance on α, it is possible to calculate how these energy levels will change if α varies.

In the vicinity of the α_0, the present day value of α, the frequency of a transition, ω, can be written as:

$$\omega = \omega_0 + qx, \tag{2.6}$$

where $x = (\frac{\alpha}{\alpha_0})^2 - 1$, ω_0 is the present day experimental value of the frequency and the q coefficient is the relativistic energy shift that determines the frequency dependence on α. It is clear from the above expression that q coefficients can be described by

$$q = \frac{d\omega}{dx}|_{x=0}.$$

Thus, in order to calculate q coefficients, the atomic energy levels of the atoms and ions of interest at different values of x need to be calculated. The relativistic energy shift, q, is then calculated using the formulae

$$q = \frac{\omega(\Delta x) - \omega(-\Delta x)}{2\Delta x} \tag{2.7}$$

and

$$q = \frac{16(\omega(\Delta x) - \omega(-\Delta x)) - 2(\omega(2\Delta x) - \omega(-2\Delta x))}{24\Delta x}. \tag{2.8}$$

The second formula is needed to check for non-linear contributions to $d\omega/dx$. We use $\Delta x = 0.1$ and $\Delta x = 0.125$. The results are presented in Table 2.2.

As for the energies, we use three different approximations to calculate relativistic energy shifts: (1) pure CI approximation for two valence electrons, (2) CI with $\hat{\Sigma}_1$ and (3) CI+MBPT approximation with both $\hat{\Sigma}_1$ and $\hat{\Sigma}_2$ included. The inclusion of core-valence correlations leads to increased values of the q-coefficients. This is because the correlation interaction of a valence electron with the core introduces an additional attraction which increases the density of the valence electron in the vicinity of the nucleus and thus acts to emphasizes the importance of the relativistic effects.

Note that $\hat{\Sigma}_1$ and $\hat{\Sigma}_2$ are of the same order and need to be included simultaneously to obtain reliable results. $\hat{\Sigma}_1$ is much easier to calculate and inclusion of $\hat{\Sigma}_1$ alone often leads to significant improvements of the results for the energies (see Table 2.1). However, the results for the q-coefficients show that neglecting $\hat{\Sigma}_2$ may lead to significant loss in accuracy. Indeed, the results for q's with $\hat{\Sigma}_1$ alone are often smaller than those obtained in pure CI and CI+MBPT approximations

Table 2.2: Calculated q coefficients (cm^{-1}), for transitions from the ground state, using H^{CI}, $H^{CI}+\hat{\Sigma}_1$ and $H^{CI}+\hat{\Sigma}_1+\hat{\Sigma}_2$

Atom/ion	State	$\hat{H}^{CI}$	$\hat{H}^{CI}+\hat{\Sigma}_1$	$H^{CI}+\hat{\Sigma}_{1,2}$	Other
AlII	$^3P_0$	138	142	146	
	$^3P_1$	200	207	211	
	$^3P_2$	325	340	343	
	$^1P_1$	266	276	278	
CaI	$^3P_0$	108	115	125	
	$^3P_1$	158	173	180	230 [34]
	$^3P_2$	260	291	294	
	$^1P_1$	228	238	250	300 [34]
SrI	$^3P_0$	384	396	443	
	$^3P_1$	560	609	642	667 [59]
	$^3P_2$	939	1072	1084	
	$^1P_1$	834	865	924	1058 [59]
InII	$^3P_0$	3230	2932	3787	4414 [36]
	$^3P_1$	4325	4125	4860	5323 [36]
	$^3P_2$	6976	7066	7767	7801 [36]
	$^1P_1$	6147	6103	6467	
YbI	$^3P_0$	2339	2299	2714	
	$^3P_1$	3076	3238	3527	
	$^3P_2$	4935	5707	5883	
	$^1P_1$	4176	4674	4951	
HgI	$^3P_0$	13231	9513	15299	
	$^3P_1$	15922	12167	17584	
	$^3P_2$	22994	19515	24908	
	$^1P_1$	20536	16622	22789	
TlII	$^3P_0$	14535	11101	16267	19745 [36]
	$^3P_1$	18476	14955	18845	23213 [36]
	$^3P_2$	32287	28903	33268	31645 [36]
	$^1P_1$	28681	25160	29418	

and differ from final values by up to 50%. Since neglecting $\hat{\Sigma}_2$ cannot be justified, we present results without $\hat{\Sigma}_2$ only for the purpose of illustration.

The accuracy of the calculation of the q-coefficients can be estimated by comparing the CI and CI+MBPT results calculated in the V^N and V^{N-2} approximations and also by comparing the final results for the energies (including the fine structure intervals) with experimental values. As one can see from Table 2.2 inclusion of the core-valence correlations can change the values of the q-coefficients by more than 15%. However, the accuracy of the energies improves significantly when core-valence correlations are included. It is natural to expect that the final accuracy for the q-coefficients is also higher when core-valence correlations are included. Comparison with our previous results also shows some deviation on approximately the same level (the largest relative discrepancy is for Ca where relativistic effects are small and high accuracy is not needed). Most of this discrepancy can be attributed to the inaccuracy of our old, less complete calculations. Comparison between the energies calculated in the V^N and V^{N-2} approximations and the experimental values suggest that 10% is a reasonable estimate of the accuracy of the present calculations of the relativistic energy shifts for Al II, Ca I and Sr I, 15% for In II, 25% for Yb I and 20% for Hg I and Tl II.

In Table 2.3 we present final values of the relativistic energy shifts together with the experimental energies.

2.4 Planning an Atomic Clock Experiment to measure α Variation

One of the factors determining the effectiveness of an atomic transition for measuring α variation is the size of the q coefficient. In Chapter 3 further factors such as line width will be considered. When planning an atomic clock experiment it

Table 2.3: Experimental energies (cm^{-1}) and calculated q-coefficients (cm^{-1}) for transitions from the ground state ns^2 to the $nsnp$ configurations of two-electron atoms/ions

Atom/Ion	Z	State		Energy[56]	q
AlII	13	$3s3p$	$^3P_0$	37393.03	146
		$3s3p$	$^3P_1$	37453.91	211
		$3s3p$	$^3P_2$	37577.79	343
		$3s3p$	$^1P_1$	59852.02	278
CaI	20	$4s4p$	$^3P_0$	15157.90	125
		$4s4p$	$^3P_1$	15210.06	180
		$4s4p$	$^3P_2$	15315.94	294
		$4s4p$	$^1P_1$	23652.30	250
SrI	38	$5s5p$	$^3P_0$	14317.52	443
		$5s5p$	$^3P_1$	14504.35	642
		$5s5p$	$^3P_2$	14898.56	1084
		$5s5p$	$^1P_1$	21698.48	924
InII	49	$5s5p$	$^3P_0$	42275	3787
		$5s5p$	$^3P_1$	43349	4860
		$5s5p$	$^3P_2$	45827	7767
		$5s5p$	$^1P_1$	63033.81	6467
YbI	70	$6s6p$	$^3P_0$	17288.44	2714
		$6s6p$	$^3P_1$	17992.01	3527
		$6s6p$	$^3P_2$	19710.39	5883
		$6s6p$	$^1P_1$	25068.22	4951
HgI	80	$6s6p$	$^3P_0$	37645.08	15299
		$6s6p$	$^3P_1$	39412.30	17584
		$6s6p$	$^3P_2$	44042.98	24908
		$6s6p$	$^1P_1$	54068.78	22789
TlII	81	$6s6p$	$^3P_0$	49451	16267
		$6s6p$	$^3P_1$	53393	18845
		$6s6p$	$^3P_2$	61725	33268
		$6s6p$	$^1P_1$	75600	29418

is important to choose a couple of atomic transitions with very different q coefficients. Ideally one would be positive and one would be negative. This would mean that if α was increasing then one of the the transition frequencies would increase and the other would decrease. Note that all q coefficients are presented for the transition to the ground state, to calculate the q coefficient for the transition between two levels which are not the ground state the q coefficients are treated in exactly the same way as the transition energies and are subtracted from each other.

In order to assist experimental atomic physicists plan appropriate experiments we have complied a list of the q coefficients calculated by our group for transitions that could be used in atomic clocks. The wavelength of the transitions rather than the energy is presented in this table to make it more immediately helpful to experimentalists. This list is presented in Appendix A. This list also highlights some interesting relationships between the q coefficients. These relationships are:

- The size of the q coefficients tend to increase with increasing atomic number, Z. This is not at all surprising since the relativistic correction to the energy level in an atom is given by [34]:

$$\Delta_n = \frac{E_n(Z\alpha)^2}{\nu}[\frac{1}{(j+1/2)} - C(Z,j,l)] \tag{2.9}$$

  where $C(Z,j,l)$ describes the contribution of many-body effects, and is usually around 0.6, ν is the effective principle quantum number, defined by $E_n = -(me^4/2\hbar^2)(Z_a^2/\nu^2)$, where the energy of the electron is E_n. Since it is only the relativistic correction to the energy level that causes it to shift as α varies it is reasonable to expect that q coefficients have the same Z^2 dependance that the relativistic correction does. The results in Table A.1 approximately follow this Z^2 dependance.

- The $s_{1/2} \rightarrow p_{1/2}$ transitions, despite having a slightly smaller energy than the $s_{1/2} \rightarrow p_{3/2}$ typically have q coefficient a lot smaller. This can be

understood by looking at Eq. 2.9, the $s_{1/2}$ and $p_{1/2}$ levels generally have a negative relativistic correction while for states with higher j such as $p_{3/2}$ the relativistic correction is positive, because of the many-body effects. Since in the $s_{1/2} \rightarrow p_{1/2}$ transition the energy levels are both moving in the same direction as α changes, we would expect the q coefficient (which tells us by how much the transition energy changes) to be smaller than in the $s_{1/2} \rightarrow p_{3/2}$ transition where the levels move apart as α changes.

- Another trend is that as α increases $s \rightarrow p$ transition energies tend to increase a little while $s \rightarrow d$ transition energies increase a lot more. This has the same explanation as above, since the $s_{1/2}$ relativistic correction is negative and the relativistic correction for d states are all positive and on average have a larger magnitude than the p states we would expect the q coefficients to follow the same trend. Note that this means that we would expect the q coefficients for a $s \rightarrow f$ transition to be even larger.

- Since Hg II has a $d \rightarrow s$ transition from the ground state (as opposed to the $s \rightarrow d$ transition in Sr II) it has a negative q coefficient.

This analysis gives us some hints about what to look for when trying to find promising transitions for measuring α variation: we should choose atoms with a large Z and hence large relativistic effects. Since transition frequencies are always measured relative to each other ideally we should have one transition with a positive q coefficient and one with a negative q coefficient, to ensure that q is large we should try and find $s \rightarrow d$ or even better, $s \rightarrow f$ transitions. Hg II is very useful since it has large Z and an unusual negative q coefficient. In Chapter 3 we will consider other things to take into account when choosing suitable atomic levels for an atomic clock experiment to measure α variation.

2.5 Conclusion

In conclusion, we have performed accurate calculations of the q coefficients, describing the size of a relativistic energy shift for many two valence electron atoms and ions. The results are presented in Table 2.3. These results are needed to place limits on a value of $\Delta\alpha/\alpha$ from measurements of the limits on a change in transition frequency over time. This measurement can be made using atomic clocks or can be deduced from absorption lines on quasar spectra.

Chapter 3

Atomic Transitions Sensitive to α Variation

There are several effects that can enhance the ability to measure a change in atomic transition frequencies with a variation of the fine structure constant, α. This chapter will investigate several possible enhancement effects. The work on using narrow lines that correspond to atomic transitions between close lying, long-lived atomic states of different configurations is my own. The rest of the chapter is a literature review, included for completeness.

My work in this chapter is based upon the paper published in The Journal of Physics B: Atomic, Molecular and Optical Physics, Angstmann *et al.* [3]

3.1 Introduction

Laboratory limits upon α variation obtained to date have all been obtained as a by-product of the study of atomic optical or microwave transitions for their use as frequency standards (atomic clocks). As a result the sensitivity of the transitions to a variation of α was not very high. The relatively low sensitivity of these

experiments to α variation is compensated for by the extremely high accuracy of the optical frequency standards. However, by carefully choosing the transitions to be measured the sensitivity to α variation can be increased [31, 34].

As discussed in Chapter 2, as α changes relativistic effects cause the energy levels in an atom to shift. If we choose close energy levels which move differently as α varies, then the size of the shift in the transition frequency compared to the size of the transition frequency will be relatively large. An extreme example of this is in dysprosium. In dysprosium there are two almost degenerate states of opposite parity with energy of 19797.97 cm^{-1}. In [34] it was demonstrated that the relative change of the transition frequency between these two levels in Dy is orders of magnitude larger than the relative change in α. An experiment is currently in progress utilizing this transition, the limit obtained to date is $\dot{\alpha}/\alpha = (-2.7 \pm 2.6) \times 10^{-15}$ per year [33, 37]. The disadvantage involved in using these levels to place limits on α variation is that they have quite a large natural linewidth, decreasing the accuracy to which the transition frequency between them can be measured.

In this chapter we consider other promising candidates to measure α variation, in particular, transitions with narrow linewidths that lie close together in the energy spectrum and will move relative to each other as α varies. The advantage of studying narrow transitions with an enhanced sensitivity is that the experiments involving these transitions should be compatible with experiments using modern optical clocks, but will involve very different systematic effects, making the results independent from the present day experiments.

3.2 Transitions with a narrow linewidth and an enhanced sensitivity to α variation

As in Chapter 2, we represent the energy of a level by

$$\omega = \omega_0 + qx \tag{3.1}$$

where $x = (\alpha/\alpha_0)^2 - 1$, ω_0 is the initial value of ω (i.e. the one measured at the beginning of the experiment) and q is a coefficient that determines the frequency dependence on a variation of α.

To determine the sensitivity of a transition to α variation we introduce an enhancement factor, κ, defined by:

$$\frac{\Delta\omega}{\omega} = \kappa\frac{\Delta\alpha}{\alpha} \tag{3.2}$$

where $\Delta\omega$ is the change in the energy, ω, of the level over the time interval separating the two measurements, and $\Delta\alpha$ is the change in α over the same period. A big value of κ obviously increases the sensitivity of the transition frequency to any variation of α. It is straightforward to show that

$$\kappa = \frac{2q}{\omega_0}. \tag{3.3}$$

When considering a pair of levels with energies ω_1 and ω_2, the enhancement factor for $\omega_2 - \omega_1$ can be written as $\kappa = \frac{2\Delta q}{\Delta\omega_0}$, where $\Delta q = q_2 - q_1$ represents the difference in the q coefficients and $\Delta\omega_0$ is the transition energy. Relativistic calculations are needed to find the values of the q coefficients and the enhancement factors. Note that κ can be positive or negative, it is negative when frequency changes and changes in α go in the opposite direction.

As discussed in Chapter 2 the measurement of the energy shift between two levels will be easiest to perform when this energy shift is large. It follows that the best situation would be to have two levels with relatively large shifts but

with opposite sign. The relative position of these two levels would change rapidly as time passed. A compromise would be to find two levels with very different q coefficients. A level with a small q coefficient will not stray much from its initial value while a level with a large q coefficient will move relatively rapidly with any change in α. The first level can then act as a reference point for the movement of the second level. As a rule of thumb the q coefficients are negative for $s_{1/2}$ and $p_{1/2}$ single electron states and positive for other states. The easiest way to ensure that two many-electron states have different q coefficients is to ensure that they have substantially different electron configurations.

In order to accurately measure any frequency shift of the transition over time it is important that the transition is narrow and systematic frequency shifts can be controlled to a high accuracy. The lifetimes of the two states involved in the transition (in particular the shorter lived state) play a major role in determining the transition width. Metastable states, from which all E1 transitions are forbidden, are ideal because of their long lifetimes. We made a very rough estimate of the lifetime of states that are not metastable by using the selection rules for an $E1$ transition to occur, namely, the parity of the final state must be opposite to the parity of the initial state and $|\Delta J| \leq 1$, in the LS coupling scheme the additional selection rules, $\Delta S = 0$ and $|\Delta L| \leq 1$ also apply. We considered all the allowed transitions from a given state to the states with lower energy. The probability of an electric dipole transition from a state i to a state j in atomic units is given by (see, for example, [60])

$$W(i \to j) = \frac{4}{3} \frac{(\alpha \omega_{ij})^3}{2J_i + 1} |A_{ij}|^2 , \tag{3.4}$$

ω_{ij} is the transition energy and J_i is the total angular momentum of the initial state. We assumed the transition amplitude, $|A_{ij}|$, is equal to 1 a.u. for our rough estimate. The lifetime of a state is then inversely proportional to the total transition probability, which is obtained by summing the transition probability of all allowed transitions.

The Lanthanides fall between the JJ coupling scheme and the LS coupling scheme and so we can expect transitions violating the approximate selection rules $\Delta S = 0$ and $|\Delta L| \leq 1$ to be suppressed but not forbidden. As an example of the accuracy that can be expected (from the assumption $|A_{ij}| = 1$) we performed the calculation for the accidentally degenerate levels in dysprosium. The calculated lifetime of the even parity state was 6.4 μs, the experimentally measured lifetime of this state is 7.9(2) μs [61]. For the odd parity state we calculated $\sim$ 700 μs, while experimentally the lifetime of this state has been measured to be greater than 200 μs [61]. We concluded that this method provides an adequate order of magnitude approximation to the lifetimes of the states. In some cases the two coupling schemes (the JJ coupling scheme where the probability amplitude of transitions between states with $\Delta S \neq 0$ is $|A_{ij}| = 1$, and the LS scheme with amplitude $|A_{ij}| = 0$ unless $\Delta S = 0$ and $|\Delta L| \leq 1$) produce significantly different answers. We can assume in these cases that the lifetime of the levels lies between these two values, but closer to the shorter one approximated using the JJ coupling scheme.

In Table 3.1 we list pairs of long-lived almost degenerate states of different configurations mainly from the rare earth elements. Here enhancement is mostly due to the small energy interval between the states. However, the fact that the configurations are different also contributes to the enhancement. Most of the transitions presented in the table correspond to $s \rightarrow d$ or $d \rightarrow f$ single-electron transitions. Since relativistic energy shifts, q, strongly depend on l and j of individual electrons [34] it is natural to expect that Δq is large for the transitions. The levels included in Table 3.1 were selected from an extensive list. We included the levels with the highest κ values that satisfied the requirements: the levels were within 100 cm^{-1} of each other, their lifetimes were both greater than 10^{-6} s, and the change of the total momentum between the levels $\Delta J \leq 2$. $\Delta J = 2$ corresponds to electric quadrupole (E2) transition in case of the same parity of

both states and magnetic quadrupole (M2) or electric octupole (E3) transition in the case of different parity. The latter might be difficult to observe, however we included one pair of such states because of a very large enhancement factor (see Table 3.1).

In Table 3.2 we list some metastable states that are close to the ground state. Here the enhancement is smaller due to the larger energy intervals. However, measurements using these levels would be easier to perform due to the convenience of dealing with transitions from the ground state.

Enhancement factors, κ, presented in Tables 3.1 and 3.2 are calculated in a single-electron approximation. We first found the relativistic energy shifts of the relevant s, p, d or f valence states of the considered atoms. This was done by varying the value of the fine structure constant α in the Hatrtree-Fock calculations (as discussed in more detail in Chapter 2). Then, transitions between real many-electron states were approximated as single electron transitions (e.g, $s-d$ or $d-f$ transitions, etc.) and the values of the relative relativistic shifts (q_1 and q_2) were found as a difference between the single-electron energy shifts of the corresponding electrons. This approach doesn't take into account configuration mixing and can be considered as a rough estimation only.

The configuration interaction can significantly change the values of κ in either direction. For example, states of the same parity and total momentum J separated by a small energy interval are likely to be strongly mixed. Therefore, the assignment of these states to particular configurations is ambiguous and the relative value of the relativistic energy shift Δq is likely to be small. An enhancement factor, κ, for such states is difficult to calculate. Its value is unstable because the transition frequency $\Delta\omega_0$ is also small. We do not include pairs of states of the same parity and momentum in Table 3.1. One can still find metastable states of the same parity and total momentum as the ground state in Table 3.2. Here mixing of states may be small due to the large energy separation between the

states.

States of the same parity but different total momentum, J, can be affected by configuration mixing in a very similar way. They can be mixed with states of appropriate values of J from other configurations. This would also bring the values of q_1 and q_2 for the two states closer to each other. On the other hand, configuration mixing can cause anomalies in the fine structure [62] or in general can have different effect on different states within the same configuration which would lead to increased sensitivity of the energy intervals to the variation of α. The detailed study of the enhancement in each listed transition goes far beyond the scope of the present work. It can be done in a much more detailed and accurate way during the planning stage of a specific experiment.

3.3 Using our calculations to plan an Experiment

By itself a large value of the enhancement factor, κ, is not enough to develop a highly sensitive search for a variation of fundamental constants. We list below the necessary conditions.

The general requirements are:

- Two levels (A and B) with different non-relativistic quantum numbers should be close to each other. Ideally at least one of the valence electrons should be in a different state, e.g., the s^2 and sd configurations. However, different many-electron states of the same configuration such as d^2 S and d^2 D could also be used, but the relativistic corrections in this case would be smaller. Close levels are levels where the relativistic separation (fine structure) is substantially bigger than the difference between the two levels A and B.

Table 3.1: Long lived almost degenerate states with large $\kappa = \frac{2\Delta q}{\Delta\omega_0}$, where $\Delta q = q_2 - q_1$. For the lifetimes, τ, M stands for metastable states and 2(-5) stands for 2×10^{-5} for example. Lifetimes are order of magnitude estimates approximated using the JJ coupling scheme. The energy levels were obtained from the NIST atomic spectral database [63].

Atom	First State				Second State				κ
or ion	Configuration		τ s	Energy cm^{-1}	Configuration		τ s	Energy cm^{-1}	
Ce I	$4f5d^26s$	$^5H_3$	M	2369.068	$4f5d6s^2$	$^1D_2$	M	2378.827	-2000
	$4f5d^26s$	$?_4$	M	4173.494	$4f5d6s^2$	$^3G_5$	M	4199.367	-800
	$4f^26s^2$	$^3H_4$	M	4762.718	$4f5d6s^2$	$^3D_2$	M	4766.323	-10000
Ce II	$4f5d6s$	$^4F_{9/2}$	2(−5)	5675.763	$4f5d^2$	$?_{7/2}$	M	5716.216	500
	$4f5d^2$	$^4S_{3/2}$	5(−4)	8169.698	$4f5d6s$	$^4D_{5/2}$	4(−5)	8175.863	-3000
Nd I	$4f^35d6s^2$	$^5K_6$	9(−6)	8411.900	$4f^45d6s$	$^7L_5$	6(−4)	8475.355	1000
	$4f^35d^26s$	$^7L_5$	2(−6)	11108.813	$4f^45d6s$	$^7K_6$	3(−5)	11109.167	10^5
	$4f^45d6s$	$^7I_7$	7(−6)	13798.860	$4f^35d^26s$	$^7K_7$	2(−6)	13799.780	$-4 \cdot 10^4$
Nd II	$4f^45d$	$^6L_{11/2}$	M	4437.558	$4f^46s$	$^4I_{13/2}$	M	4512.481	-300
	$4f^45d$	$^6G_{11/2}$	2(−4)	12021.35	$4f^46s$	$^6F_{9/2}$	6(−4)	12087.17	-300
Sm I	$4f^66s^2$	$^5D_1$	7(−5)	15914.55	$4f^65d6s$	$^7G_2$	2(−4)	15955.24	500
Eu I	$4f^76s6p$	$^{10}P_{11/2}$	2(−4)	15581.58	$4f^75d6s$	$^8D_{9/2}$	9(−4)	15680.28	100
Gd II	$4f^75d6s$	$^8D_{11/2}$	M	4841.106	$4f^75d^2$	$^{10}F_{9/2}$	M	4852.304	2000
	$4f^75d^2$	$^{10}P_{7/2}$	0.1	10599.743	$4f^75d6s$	$^6D_{5/2}$	M	10633.083	-600
Tb I	$4f^96s^2$	$^6H_{13/2}$	2(−4)	2771.675	$4f^85d6s^2$	$^8G_{9/2}$	M	2840.170	-600
Tb II	$4f^85d6s$	$?_6$	7(−5)	5147.23	$4f^96s$	$?_6$	5(−4)	5171.76	2000

Table 3.2: Metastable states sensitive to variation of α. The energy levels were obtained from the NIST atomic spectral database [63].

Atom		Ground State			Metastable State				κ
or ion	Z	Configuration		J	Configuration		J	Energy (cm^{-1})	
La I	57	$5d6s^2$	^{2}D	3/2	$5d^26s$	^{4}F	5/2	3010.002	7
					$5d^3$	^{4}F	3/2	12430.609	3
La II	57	$5d^2$	^{3}F	2	$5d6s$	^{3}D	1	1895.15	-10
					$6s^2$	^{1}S	0	7394.57	-5
Ce II	58	$4f5d^2$	^{4}H	7/2	$4f5d6s$		9/2	2382.246	-8
Pr I	59	$4f^36s^2$	^{4}I	9/2	$4f^35d6s$	^{6}L	11/2	8080.49	2
Pr II	59	$4f^36s$		4	$4f^35d$	^{5}L	6	3893.46	5
Nd I	60	$4f^46s^2$	^{5}I	4	$4f^45d6s$	^{7}L	5	8475.355	3
Nd II	60	$4f^46s$	^{6}I	7/2	$4f^45d$	^{6}L	11/2	4437.558	5
Sm I	62	$4f^66s^2$	^{7}F	0	$4f^65d6s$	^{9}H	1	10801.10	2
Sm II	62	$4f^66s$	^{8}F	1/2	$4f^65d$	^{8}H	3/2	7135.06	3
Eu I	63	$4f^76s^2$	^{8}S	7/2	$4f^75d6s$	^{10}D	5/2	12923.72	2
Eu II	63	$4f^76s$	^{9}S	4	$4f^75d$	^{9}D	2	9923.00	2
Gd I	64	$4f^75d6s^2$	^{9}D	2	$4f^75d^26s$	^{11}F	2	6378.146	3
Gd II	64	$4f^75d6s$	^{10}D	5/2	$4f^76s^2$	^{8}S	7/2	3444.235	-6
Tb I	65	$4f^96s^2$	^{6}H	15/2	$4f^85d6s^2$	^{8}G	13/2	285.500	-100
Pt I	78	$5d^96s$	^{3}D	3	$5d^86s^2$	^{4}F	4	823.7	-20
Pt II	78	$5d^9$	^{2}D	5/2	$5d^86s$	^{4}F	9/2	4786.6	-6
Ac III	89	$7s$	^{2}S	1/2	$6d$	^{2}D	3/2	801.0	20
					$6d$	^{2}D	5/2	4203.9	5

- The levels must be narrow and the systematic frequency shifts of the transition frequency must be small, enabling an accurate determination of the transition frequency. The ratio of the relative measurement uncertainty, $\delta\omega/\omega$, to the enhancement factor, κ, can be considered as a characteristic value for comparison with other searches for α variation.

- It should be possible to induce a transition between the states A and B, and there should an efficient tool to detect the transition. Cooling the atoms is essential in order to increase the accuracy of the frequency measurements.

The number of successful detection and cooling schemes for precision spectroscopy is quite limited and this leads to strong limitations on candidates. However, recent progress in "quantum-logic" spectroscopy [64, 65] opens up new possibilities for the cooling and high-resolution spectroscopy of a large number of ions.

The advantages of the enhancement are twofold. Firstly, one can make a measurement with a reduced accuracy and still reach a competitive result. This allows one to get rid of certain systematic effects present in most precision measurements. Secondly, if a high precision measurement is possible (as we hope in the case of some of the narrow transitions) the enhancement may offer the strongest test possible in a laboratory study.

3.4 Other Methods of Enhancing the Energy Shift

Members of our group have been investigating other situations in which a variation of α is enhanced (i.e. $\kappa > 1$). Below is a summary of several of the promising situations they have found. As discussed above all measurements of α variation made so far (apart from the one utilizing the degenerate lines in dysprosium, currently being conducted by Cingöz *et al.* [37]) using atomic clocks have come

about from very accurate measurements of atomic frequency standards. The transitions have been chosen for their appropriateness as frequency standards, which means that they have a very high accuracy, rather than for any enhancement of α variation, which could possibly give a better limit on changes in α variation even with decreased accuracy in the measurements.

3.4.1 Fine Structure Anomalies

In [62] Dzuba and Flambaum suggest using anomalously small fine structure intervals in the ground state (or very low excited states) of many electron atoms. For "normal" fine-structure intervals $\kappa = 2$ (there is no fine structure for $\alpha = 0$ and the fine structure intervals are proportional to $(Z\alpha)^2$ so $\Delta q = \omega_0$ and so $\kappa = 2$ follows from Eq. 3.3). However, in some atoms the fine structure interval is strongly perturbed by the configuration interaction with neighbouring states. This can result in an anomalously small fine structure interval that in turn can lead to an increased enhancement factor. Dzuba and Flambaum found an enhancement factor of 106 between the $^3P_1$ and $^3P_0$ states of the fine structure multiplet in Te I. Using ground state fine structure multiplets has an additional advantage, the states are metastable, they can only decay by an M1 transition which is suppressed because of the small transition frequency. As a consequence the lines are very narrow allowing very accurate measurements to be taken. These anomalies are not unusual (although the energy interval in Te I is exceptionally small), practically all elements with the np^4 configuration have anomalies in the fine structure [62].

3.4.2 Narrow transition in the ^{229}Th nucleus

In [66] Flambaum suggests using a very narrow ultraviolet transition between the ground state and the first excited state in the ^{229}Th nucleus to measure variation

of constants, including α, because of the 5-6 order of magnitude enhancement here. In this work Flambaum shows that:

$$\frac{\delta\omega}{\omega} \approx 10^5(4\frac{\delta\alpha}{\alpha} + \frac{\delta X_q}{X_q} - 10\frac{\delta X_s}{X_s})\frac{3.5 \text{ eV}}{\omega},$$

where $X_q = m_q/\Lambda_{QCD}$ and $X_s = m_s/\Lambda_{QCD}$. There were several approximations made in obtaining the result but for the most important implication of this result these are unimportant: variation of α is enhanced by 5 orders of magnitude ($\kappa = 4 \times 10^5$). Another advantage of using this transition is that the width of the transition is several orders of magnitude narrower than typical atomic clock widths ($\sim 1 - 100$ Hz) [66], it can be investigated with laser spectroscopy.

3.4.3 Diatomic molecules with unpaired electrons

In [67] Flambaum suggests using microwave transitions between very close and narrow rotational-hyperfine levels in diatomic molecules with unpaired electrons such as LaS, LaO, LuS, LuO and YbF. In this case the enhancement comes about due to the cancelation between hyperfine and rotational intervals. Flambaum shows that in this case the enhancement factor, κ is given by:

$$\kappa = \frac{4b}{\omega}(2 + K),$$

where b is the hyperfine structure constant, and $K = \frac{(Z\alpha)^2(12\gamma^2-1)}{\gamma^2(4\gamma^2-1)}$ where $\gamma = \sqrt{1-(Z\alpha)^2}$ (Z refers to the nuclear charge of the heavier atom). Flambaum estimates that κ would be around 600 but accurate measurements of the transtion frequency, ω, are needed to get an accurate value of κ.

3.5 Conclusion

There are a number of effects that can enhance the sensitivity of some transitions to a variation of α and it is possible to use these transitions to obtain a tighter

limit on the variation of α than is otherwise possible. We have presented a number of transitions between narrow states of many-electron atoms with large enhancement of the change of the frequency of the transitions due to the change of α. The enhancement factors for atomic clock transitions which have been used in the search for variation of α were rather small ($\kappa \sim 1$ or even smaller). This suggests that it should be possible to obtain a much tighter constraints on α variation even without technical improvements in frequency metrology, by instead carefully choosing the transition frequencies to investigate.

Chapter 4

Varying Constant or a New Interaction?

In early 2003 Bekenstein published an article on the pre-print archives [68] that cast some doubt over the method used by all the groups who measure limits upon fine structure constant (α) variation from quasar spectra [15–17]. Implicit in the method put forward in Dzuba *et al.* [34, 69] and subsequently used by all the groups investigating α variation in quasar spectra is the assumption that the value of α in the past can be determined by first of all compensating for the redshift, z, and then fitting the value of α to the spectrum using the same equations as would be used for a laboratory spectrum. Bekenstein points out that in performing this operation we make the assumption that the *form* of the Dirac Hamiltonian has not changed between when the light was emitted and now, when it is observed. He questions the validity of this assumption. We showed that in fact if the Dirac equation is modified in the way suggested by Bekenstein, the analysis used by the groups investigating α variation is still correct since the effect of the modified form of the Dirac Hamiltonian is indistinguishable from a small change in α.

The work presented in this chapter is based upon the Physical Review A publication Angstmann *et al.* [2].

4.1 Introduction

Bekenstein showed that a dynamically varying α can be considered as a perturbation of the Dirac Hamiltonian, $\hat{H}$, for an electron bound by a Coulomb field (unfortunately no self-consistent quantum electrodynamic theory was derived):

$$\hat{H} = \hat{H}_0 + \delta\hat{H} \tag{4.1}$$

$$\hat{H}_0 = (-\imath\hbar c\boldsymbol{\alpha}\cdot\boldsymbol{\nabla} + mc^2\beta + eV_C I) \tag{4.2}$$

$$\delta\hat{H} = (I-\beta)(\tan^2\chi)V_C \tag{4.3}$$

where $V_C = -Ze^2/r$, I is the identity matrix. The last term is related to an effective correction to the Coulomb field due to the dynamic nature of α, and $\tan^2\chi$ is a small parameter. The perturbative term, $\delta\hat{H}$, vanishes in a non-relativistic approximation but produces some relativistic corrections which can be studied both in astrophysical spectra and laboratory conditions.

In the following sections we will show how this perturbation shifts atomic energy levels. In particular we pay attention to heavy atoms which provide us with astrophysical data and are the most sensitive to a possible α variation. We also consider atomic hydrogen, since it is the best understood atomic system for laboratory experiments.

4.2 Multielectron Atoms

Multielectron atoms are of interest to us since they are the most sensitive to a varying α. We performed a calculation to show how the modified form of the Dirac Hamiltonian affects the energy of an external electron in a heavy atom. The most convenient way to calculate δE is to calculate the matrix element of the operator $\delta\hat{H} = (I-\beta)\tan^2\chi\cdot V_C$ for an external electron in a many-electron atom or ion using a relativistic wave function. In order to use the relativistic wave functions for electrons near the nucleus at zero energy it is necessary to

demonstrate that the major contribution to the matrix element of $\delta\hat{H}$ comes from distances $r \lesssim a/Z$, a is the Bohr radius of the atom, where the screening of the nuclear potential and the external electron energy can be neglected. We will show that only the contribution at distances $r \lesssim a/Z$ has a Z^2 enhancement, the contribution at $r \sim a$ does not have this enhancement since the atomic potential at this distance is screened, $V_C \sim e^2/r$, and has no Z dependence. To demonstrate the Z^2 enhancement of the $r \lesssim a/Z$ contribution let us consider the non-relativistic limit of the operator $\delta\hat{H}$. The matrix

$$I - \beta = \begin{pmatrix} 0 & 0 \\ 0 & -2 \end{pmatrix}$$

has only lower components, it follows that the matrix element,

$$\psi^+(I-\beta)V_C\psi = -2\chi^+V_C\chi, \tag{4.4}$$

where

$$\psi = \begin{pmatrix} \varphi \\ \chi \end{pmatrix}$$

is the Dirac spinor. In the non-relativistic limit

$$\chi = \frac{\boldsymbol{\sigma}\cdot\mathbf{p}}{2mc}\varphi$$

and this gives

$$\delta\hat{H} = -\frac{1}{2m^2c^2}(\boldsymbol{\sigma}\cdot\mathbf{p})V_C(\boldsymbol{\sigma}\cdot\mathbf{p})\tan^2\chi. \tag{4.5}$$

We proceed with the derivation in a very similar fashion to the standard derivation of the spin-orbit interaction term in the non-relativistic expansion of the Dirac Hamiltonian (see [60] for example)

$$\delta\hat{H} \approx \Big(- V_C\frac{p^2}{2m^2c^2} + \frac{i\hbar}{2m^2c^2}(\nabla V_C\cdot\mathbf{p}) - \frac{\hbar^2}{2m^2c^2}\frac{1}{r}\frac{dV_C}{dr}\boldsymbol{\sigma}\cdot\mathbf{l}\Big)\tan^2\chi. \tag{4.6}$$

Let us now compare the contributions of $r \lesssim a/Z$ and $r \sim a$ to the matrix element of $\delta\hat{H}$. Consider, for example, the last spin-orbit term in Eq. (4.6) which

is proportional to the usual spin-orbit interaction. The electron wave function at $r \sim a/Z$ is given by $\varphi^2 \sim Z/a^3$ [70], the spin-orbit operator is proportional to

$$\frac{1}{r}\frac{dV_C}{dr} \sim \frac{1}{r^3} Ze^2$$

and the integration volume is proportional to r^3. As a result we can write:

$$< \delta\hat{H} > \sim Z^2 \frac{\hbar^2 e^2}{2m^2c^2a^3}. \tag{4.7}$$

For $r \sim a$, the wave function is $\varphi^2 \sim 1/a^3$, the spin-orbit operator is proportional to

$$\frac{1}{r}\frac{dV_C}{dr} \sim \frac{1}{r^3} e^2$$

and the integration volume is still proportional to r^3. Therefore

$$< \delta\hat{H} > \sim \frac{\hbar^2 e^2}{2m^2c^2a^3}, \tag{4.8}$$

this is Z^2 times smaller than at $r \lesssim a/Z$. The same conclusion is also valid for the first two terms in Eq. (4.5). This estimate demonstrates that the main contribution to $\delta\hat{H}$ comes from small distances $r \lesssim a/Z$. This conclusion is similar to that for the relativistic corrections to atomic electron energy.

We perform the actual calculation of the matrix element of $\delta\hat{H}$ using the relativistic Coulomb wave functions for zero-energy electrons near the nucleus. These can be expressed in terms of Bessel functions as (these wave functions can be found in [71]):

$$\begin{aligned} f_{njl}(r) &= \frac{c_{njl}}{r}\Big((\gamma+\kappa)J_{2\gamma}(x) - \frac{x}{2}J_{2\gamma-1}(x)\Big) \\ g_{njl}(r) &= \frac{c_{njl}}{r} Z\alpha J_{2\gamma}(x) \end{aligned} \tag{4.9}$$

where $x = (8Zr/a)^{1/2}$, $\gamma = \sqrt{(j+1/2)^2 - Z^2\alpha^2}$, $\kappa = (-1)^{j+1/2-l}(j+1/2)$ and

$$c_{njl} = \frac{\kappa}{|\kappa|}\Big(\frac{1}{Za\nu^3}\Big)^{1/2} Z_a,$$

here Z_a is the charge"seen" by the external electron, i.e. $Z_a = 1$ for a neutral atom, 2 for a singly ionized atom and Z for a hydrogen-like ion and ν is the

effective principle quantum number, defined by $E_n = -(me^4/2\hbar^2)(Z_a^2/\nu^2)$, where the energy of the electron is E_n; for hydrogenlike ions, $\nu = n$. δE can now be calculated using these wave functions and $\delta\hat{H}$:

$$\begin{aligned}
\delta E &= \int \psi^+ \delta\hat{H}\psi dV \\
&= -2\tan^2\chi \int_0^\infty g^+_{njl} V_C g_{njl} r^2 dr \\
&= -2e^2Z^3\alpha^2\tan^2\chi c^2_{njl}\int_0^\infty J^2_{2\gamma}(x)\frac{dr}{r} \\
&= -4e^2Z^3\alpha^2\tan^2\chi c^2_{njl}\int_0^\infty J^2_{2\gamma}(x)\frac{dx}{x}.
\end{aligned}$$

We now use the relationships between Bessel functions and Gamma functions to write this as:

$$\begin{aligned}
\delta E &= -2e^2Z^3\alpha^2\tan^2\chi c^2_{njl}\frac{\Gamma(2\gamma)}{\Gamma(2\gamma+1)} \\
&= -\frac{e^2Z^3\alpha^2\tan^2\chi c^2_{njl}}{\gamma}.
\end{aligned}$$

When we substitute in for c_{njl} we obtain:

$$\delta E = -\frac{mc^2Z^2Z_a^2\alpha^4\tan^2\chi}{\nu^3\gamma}.$$

Finally, we take the non-relativistic limit by replacing γ with $j + 1/2$,

$$\delta E = -\frac{mc^2Z^2Z_a^2\alpha^4\tan^2\chi}{\nu^3(j+1/2)}. \tag{4.10}$$

By dividing this equation by the energy of the electron, $E = -Z_a^2mc^2\alpha^2/(2\nu^2)$, we obtain the result:

$$\frac{\delta E}{E} = \frac{2(Z\alpha)^2\tan^2\chi}{\nu}\frac{1}{j+1/2}. \tag{4.11}$$

It is interesting to note that this correction to the energy of the electron has exactly the same form as the relativistic correction, Δ, to the energy of an external electron:

$$\frac{\Delta}{E} = \frac{(Z\alpha)^2}{\nu}\frac{1}{j+1/2}. \tag{4.12}$$

Note that to obtain Eq. (4.11) we simply divided Eq. (4.10) by $E = -Z_a^2 m\alpha^2/(2\nu^2)$, the spin-orbit contribution to Eq. (4.12) can be obtained in an analogous manner. We can sum up Bekenstein's relativistic correction, Eq. (4.11), and the usual relativistic correction to give

$$\frac{\Delta'}{E} \simeq \frac{(Z\alpha')^2}{\nu}\frac{1}{j+1/2}. \tag{4.13}$$

where $\alpha' = \alpha(1+\tan^2\chi)$.

Finally, we should present a very simple derivation of Eqs. (4.11) and (4.12) based on the results obtained for the pure Coulomb case, see Eqs. (4.16) and (4.17). For the high electron orbitals ($n \gg 1$) the electron energy at $r \sim a/Z$ may be neglected in comparison with the Coulomb potential and the Coulomb results Eqs. (4.16) and (4.17) are proportional to the electron density at $r \sim a/Z$ where $\psi^2 \sim 1/n^3$. For the external electron in heavy atoms the situation is similar. The external electron wave function in Eqs. (4.9) at $r \sim a/Z$ is proportional to the Coulomb wave function for small energy ($n \gg 1$). Therefore, to find the matrix elements for the external electron we should take the Coulomb results Eqs. (4.16) and (4.17) and multiply them by the ratio of the electron densities for the external electron in the many-electron atom and the Coulomb electron. This immediately gives Eqs. (4.11) and (4.12).

The works [15–17] used a method suggested in [69] for the analysis of absorption lines. A comparison between different frequencies is used. In this method only the relativistic corrections, Δ'/E, are used to determine α variation since any variation in the energy in the non-relativistic limit is absorbed into the redshift parameter (and it also scales the same way for all elements). Since Eq. (4.11) and (4.12) are directly proportional, the effect of the modified form of the Dirac Hamiltonian is indistinguishable from a small change in α^2 in Eq. (4.12). A measurable change in α would in fact be a change of $\alpha' = \alpha(1+\tan^2\chi)$. The astrophysical data can not distinguish between α and $\tan^2\chi$ variation.

Note that the proportionality of δE and Δ has a simple explanation. The

relativistic corrections to the Schrödinger Hamiltonian (e.g. the spin-orbit interaction) and the non-relativistic limit of $\delta\hat{H}$ have similar dependence on r and both are proportional to the electron density ψ^2 at $r \sim a/Z$. The proportionality of δE and Δ also holds for high orbitals (small binding energy) in the pure Coulomb case (see next section).

In this derivation we assumed that we could consider the unscreened Coulomb field, this is clearly not the case for a valence electron in a many-electron atom. We justify this assumption by once again noting that the main contribution to δE is given by distances close to the nucleus, $r \sim a/Z$. At this distance the main screening comes from the $1s$ electrons and we can use Slater's rules [72, 73] to estimate the screening corrections to Eq. (4.11) and (4.12):

$$\frac{\delta E}{E} = \frac{2\alpha^2(Z-0.6)^2\tan^2\chi}{\nu}\frac{1}{j+1/2} \tag{4.14}$$

$$\frac{\Delta}{E} = \frac{\alpha^2(Z-0.6)^2}{\nu}\frac{1}{j+1/2}. \tag{4.15}$$

This does not affect the proportionality of the two terms and makes very little difference to the results in heavy atoms ($\sim 1/Z$). The correction from the non-zero energy of the external electron is even smaller ($\sim 1/Z^2$). Consideration of many-body correlation corrections has shown that this does not change the proportionality relationship either. The point is that the expressions for the correlation corrections obtained using the many-body perturbation theory (or the configuration interaction method) contain the single-particle matrix elements of $\delta\hat{H}$ and that of the relativistic corrections which are proportional to each other. This makes the final results proportional. Because of this proportionality it is not possible to derive values for α and $\tan^2\chi$ separately in mulitelectron atoms. However, a separation of these values can be achieved in hydrogen.

4.3 Calculations Involving the Hydrogen Atom

The case is somewhat simplified for the hydrogen atom and other hydrogen-like ions as there are no inter-electron interactions. There are also very accurate experimental measurements of transition frequencies in hydrogen.

We confirm Bekenstein's result [68] that applying the Hamiltonian (4.1) one can derive:

$$\delta E = -\frac{mc^2 Z^4 \alpha^4}{n^3}\left(\frac{1}{j+1/2} - \frac{1}{2n}\right)\tan^2\chi\,. \tag{4.16}$$

The relativistic correction to the electron energy is

$$\Delta = -\frac{mc^2 Z^4 \alpha^4}{2n^3}\left(\frac{1}{j+1/2} - \frac{3}{4n}\right). \tag{4.17}$$

Note that for large n (zero energy), δE is again proportional to the relativistic correction, Δ.

It is possible to obtain a limit on the $\tan^2\chi$ parameter by comparing the theoretical and experimental data for the $2p_{3/2}-2p_{1/2}$ splitting. The experimental value

$$f_{2p_{3/2}\to 2p_{1/2}}(\text{exp}) = 10\,969\,045(15)\,\text{kHz} \tag{4.18}$$

is derived from two experimental results,

$$f_{2s_{1/2}\to 2p_{3/2}}(\text{exp}) = 9\,911\,200(12)\,\text{kHz} \tag{4.19}$$

$$f_{2p_{1/2}\to 2s_{1/2}}(\text{exp}) = 1\,057\,845(9)\,\text{kHz} \tag{4.20}$$

presented in [74] and [75] respectively. It can be compared to the theoretical value which we take from a compilation [76] (see also review [77])

$$f_{2p_{3/2}\to 2p_{1/2}}(\text{theory}) = 10\,969\,041.2(15)\,\text{kHz}\,. \tag{4.21}$$

Noting that δE has not been accounted for in the Eq. (4.21), but will be present in Eq. (4.18), and using Eq. (4.16) we can write:

$$\frac{mc^2\alpha^4}{16h}\tan^2\chi = f_{2p_{3/2}\to 2p_{1/2}}(\text{exp}) - f_{2p_{3/2}\to 2p_{1/2}}(\text{theory}). \tag{4.22}$$

Dividing all the terms by $f_{2p_{3/2}\to 2p_{1/2}}(\text{theory})$ and noting that the leading contribution to $f_{2p_{3/2}\to 2p_{1/2}}(\text{theory})$ is given by $mc^2\alpha^4/32h$, allows us to write:

$$f_{2p_{3/2}\to 2p_{1/2}}(\text{exp}) = \text{f}_{2\text{p}_{3/2}\to 2\text{p}_{1/2}}(\text{theory})(1 + 2\tan^2\chi) \tag{4.23}$$

Using the values above we can obtain the limit $\tan^2\chi = 2(7)\times 10^{-7}$. It is assumed here that $f_{2p_{3/2}\to 2p_{1/2}}(\text{theory})$ is expressed in terms of α which is extracted from the measurements of parameters which are not sensitive to $\tan^2\chi$ (i.e. they depend on α rather than on α'). Indeed, one of the values of α is derived via a complicated chain of relations with α eventually coming from the Rydberg constant which is quite weakly affected by $\delta\hat{H}$ (the relative value of the correction is of order of $\alpha^2\tan^2\chi$ since the matrix element of $\delta\hat{H}$ vanishes in a leading non-relativistic approximation). The most accurate result obtained this way is $\alpha^{-1} = 137.036\,000\,3(10)$ [78].

A self consistent quantum electrodynamic theory with a dynamically varying α should meet some even stronger constraints due to a comparison of the value of the fine structure constant from the anomalous magnetic moment of the electron ($\alpha^{-1} = 137.035\,998\,80(52)$ [79]) with the Rydberg constant value. Such a comparison will likely lead to a limitation on $\tan^2\chi$ at a level of a few parts in 10^{-8} since $\delta\alpha/\alpha = 11(8)\times 10^{-9}$, from comparison of the values for α^{-1} given above.

Before any modification of QED due to a varying α can be seriously considered another set of questions need to be answered. These questions should target its gauge invariance, renormalizability and Ward identities, which supports the same charge for electrons and protons. The current QED construction is quite fragile and it is not absolutely clear if it can be successfully extended.

4.4 Conclusion

In conclusion, using the modified form of the Dirac Hamiltonian Eqs. (4.1)-(4.3) does not affect the analysis used in [13, 15–17, 80]. They measure the variation of $\alpha' = \alpha(1 + \tan^2\chi)$. The present time limit $\tan^2\chi = (0.2 \pm 0.7) \times 10^{-6}$ is obtained from the measurement of the hydrogen $2p$ fine structure using value of α obtained from different experiments. Note that according to [15] the value of α' was smaller in the past, the last measurement gave $\Delta\alpha'/\alpha' = (-0.54 \pm 0.12) \times 10^{-5}$. If there is no other source of variation of α (i.e if any change in α was in fact a change in $\tan^2\chi$) this would require a negative value of $\tan^2\chi$ ($\tan^2\chi = (-0.52 \pm 0.14) \times 10^{-5}$) since the present value of $\tan^2\chi$ is small. Actually, the choice of the integration constants in the Bekenstein paper precludes considering epochs with $\alpha' < \alpha$ [68], however, this should not be deemed a principle problem.

In summary if a variation of α does perturb the Dirac Hamiltonian in the way suggested by Bekenstein (which is by no means certain) then the method used to determine α variation from quasar spectra and atomic clocks is still valid. The only modification is that a measurement of $\Delta\alpha/\alpha$ is in fact a measurement of $\Delta\alpha'/\alpha'$ where $\alpha' = \alpha(1 + \tan^2\chi)$.

Chapter 5

Frequency shifts caused by Blackbody Radiation

When searching for evidence of fine structure constant, α, variation using atomic clocks it is necessary to take into account other corrections that will change the transition frequencies and decrease the accuracy to which a measurement of a limit on α variation can be made. One of the major contributors to the uncertainty in measurements of transition frequencies made with atomic clocks is a small frequency shift caused by blackbody radiation. We have performed calculations of the size of the frequency shift induced by a static electric field (present due to blackbody radiation) on the clock transition frequencies of the hyperfine splitting in Yb^+, Rb, Cs, Ba^+, and Hg^+. The calculation of the frequency shift in Cs is of particular interest because this shift needs to be known to accurately determine the length of a second. This work is important because it explains the discrepancies between previous calculations of the correction to the blackbody cesium frequency shift; the difference ($\sim 10\%$) between *ab initio* and semiempirical calculations is due to the contribution of the continuum spectrum in the sum over intermediate states, when these states are included all the results are brought into agreement.

The work presented in this chapter is based upon the work presented in the Physical Review A article, Angstmann *et al.* [5] and the Physical Review Letter, Angstmann *et al.* [4].

5.1 Introduction

The hyperfine structure (hfs) transition of the ground state of ^{133}Cs serves as a primary frequency standard, providing the definition of a metric second. The definition of the second is:
"The second is the duration of 9 192 631 770 periods of the radiation corresponding to the transition between the two hyperfine levels of the ground state of the caesium 133 atom."
At its 1997 meeting the Comitè international des poids et mesures (CIPM) affirmed that this definition referred to "the cesium atom at rest at a temperature of 0K", in other words the definition of the second refers to a cesium atom unperturbed by blackbody radiation so measurements of the second need to correct for this perturbation.

Many other similar hfs transitions in other atoms and ions are used or are under consideration for use as secondary microwave frequency standards. Most frequency standards (atomic clocks) operate at room temperature. This means that readings from atomic clocks should be corrected to account for the effect of blackbody radiation (see, e.g., Ref. [81]) so that they can be directly compared to each other. The value of this effect can be found from measurements or calculations. There are many experimental [82–87] and theoretical [81, 88–93] works studying the effects of blackbody radiation on microwave frequency standards. However, the situation is far from being satisfactory. There is disagreement among the different works for cesium which we will discuss in more detail, while the data for other atoms and ions is very poor or absent.

Early measurements of the radiation frequency shift in cesium [82, 83, 85] and *ab initio* calculations [89, 90] support a value of $\delta\nu_0$ which is close to $-2.2 \times 10^{-10}\mathrm{Hz/(V/m)^2}$ while more recent measurements [86, 87] and semiempirical calculations [88, 91, 92] claim that the actual number might be about 10% smaller. While we can not comment on the experimental results, the source of the disagreement between theoretical values seems to be in the continuum spectrum.

We have performed fully *ab initio* calculations of the radiation frequency shift and have identified the source of the disagreement between different theoretical results as the contribution of the continuum spectrum states into summation over the complete set of intermediate states. The continuum spectrum was included in all the *ab initio* calculations and missed in the semiempirical considerations. We demonstrate that by adding the contribution of the continuum spectrum to where it was missed we bring all theoretical results into good agreement with each other and with early measurements.

5.2 Theory

Blackbody radiation creates a temperature dependent electric field, described by the Planck radiation law

$$E^2(\omega) = \frac{8\alpha}{\pi} \frac{\omega^3 d\omega}{\exp(\omega/kT) - 1}. \tag{5.1}$$

This leads to the following expression for the average electric field radiated by a black body at temperature T:

$$\langle E^2 \rangle = (831.9\mathrm{V/m})^2[\mathrm{T(K)}/300]^4. \tag{5.2}$$

This electric field causes a temperature-dependent frequency shift of the atomic microwave clock transitions. It can be presented in the form (see, e.g. [81])

$$\delta\nu/\nu_0 = \beta(T/T_0)^4 \left[1 + \epsilon(T/T_0)^2\right]. \tag{5.3}$$

Here T_0 is usually assumed to be room temperature ($T_0 = 300K$). The frequency shift in a static electric field is

$$\delta\nu = kE^2. \tag{5.4}$$

Coefficients k and β (in Eqs. (5.4) and (5.3)) are related by

$$\begin{aligned} \beta &= \frac{k}{\nu_0}(831.9\mathrm{V/m})^2 \\ &= k \times 7.529 \times 10^{-5}(\mathrm{V/m})^2\mathrm{Hz}^{-1} \quad \text{(for Cs)}, \end{aligned} \tag{5.5}$$

where ϵ is a small correction due to the frequency distribution (5.1). We have calculated the coefficients k, β and ϵ.

It is convenient to start the calculation of k by considering an atom in a static electric field. In the case with no other external electric field to set a preferred direction, the radiation shift can be expressed in terms of the scalar hyperfine polarizability of the atom. This corresponds to averaging over all possible directions of the electric field. The hyperfine polarizability is the difference of the atomic polarizabilities between different hyperfine structure states of the atom. The lowest-order effect is linear in the hyperfine interaction and quadratic in the electric field. Therefore, its value can be calculated using third-order perturbation theory (see, e.g. [70])

$$\delta\epsilon_a = \sum_{n,m} \frac{\langle a|\hat{V}|n\rangle\langle n|\hat{V}|m\rangle\langle m|\hat{V}|a\rangle}{(\epsilon_a - \epsilon_n)(\epsilon_a - \epsilon_m)} - \langle a|\hat{V}|a\rangle \sum_n \frac{\langle a|\hat{V}|n\rangle^2}{(\epsilon_a - \epsilon_n)^2}. \tag{5.6}$$

In our case the perturbation operator $\hat{V}$ is the sum of the hyperfine structure operator and the electric dipole operator

$$\hat{V} = \hat{H}_{hfs} - e\boldsymbol{E}\cdot\boldsymbol{r}.$$

The operator of the hyperfine interaction $\hat{H}_{hfs}$ is given by

$$\hat{H}_{hfs} = \frac{|e|}{c}\boldsymbol{\mu}\cdot\frac{\boldsymbol{r}\times\boldsymbol{\alpha}}{r_>^3}, \quad r_> = \max(r, r_N), \tag{5.7}$$

where $\boldsymbol{\alpha}$ is the Dirac matrix, $\boldsymbol{\mu}$ is the magnetic moment of the nucleus and r_N is nuclear radius.

To get the effect of the electric field on the frequency of the hyperfine transition one needs to go through the following steps:

- Substitute the perturbation operator $\hat{V}$ into equation (5.6).
- Keep only terms linear in $\hat{H}_{hfs}$ and quadratic in the electric field.
- Apply equation (5.6) to both components of the hyperfine structure doublet.
- Take the difference.

The resulting expression for the frequency shift consists of three terms. The first two of them originate from the first term of equation (5.6). In one of them the $\hat{H}_{hfs}$ operator is either on the left or right side of the expression (these two terms are equal and can be combined together), and in the other the $\hat{H}_{hfs}$ operator is in the middle. The last term is due to change of the normalization of the wave function (second term of equation (5.6)). It is proportional to the hyperfine structure of the ground state.

After angular reduction these three terms become

$$\delta\nu_1(as) = e^2\langle E^2\rangle \frac{2I+1}{6} \times \sum_{n,m,j} \frac{A_{as,ns}\langle ns||r||mp_j\rangle\langle mp_j||r||as\rangle}{(\epsilon_{as}-\epsilon_{ns})(\epsilon_{as}-\epsilon_{mp_j})}, \tag{5.8}$$

$$\delta\nu_2(as) = \frac{e^2\langle E^2\rangle}{6} \sum_j (C_{I+1/2} - C_{I-1/2}) \times \sum_{n,m} \frac{\langle as||r||npj\rangle A_{npj,mpj}\langle mp_j||r||as\rangle}{(\epsilon_{as}-\epsilon_{npj})(\epsilon_{as}-\epsilon_{mp_j})}, \tag{5.9}$$

and

$$\delta\nu_{norm}(as) = -e^2\langle E^2\rangle \frac{2I+1}{12} A_{as} \sum_{m,j} \frac{|\langle as||r||mp_j\rangle|^2}{(\epsilon_{as}-\epsilon_{mp_j})^2}. \tag{5.10}$$

Here

$$C_F = \sum_{F'} (2F'+1)[F'(F'+1) - I(I+1) - j(j+1)]$$
$$\times \left\{ \begin{array}{ccc} 1/2 & F & I \\ F' & j & 1 \end{array} \right\}^2, \quad F' = |I-J|, I+J,$$

A_{ns} is the hfs constant of the ns state, $A_{m,n}$ is the off-diagonal hfs matrix element, I is nuclear spin, $\mathbf{F} = \mathbf{I} + \mathbf{J}$, $\mathbf{J}$ is total electron momentum of the atom in the ground state ($J = 1/2$ for atoms considered here), and j is total momentum of virtual p-states ($j = 1/2, 3/2$). Summation goes over a complete set of ns, $mp_{1/2}$ and $mp_{3/2}$ states.

Expression (5.8) does not include the $s-d$ hfs matrix elements while expression (5.9) does not include the $p_{1/2} - p_{3/2}$ hfs matrix elements. Test calculations show that the total contribution of the off-diagonal (in total momentum j) hfs matrix elements is of the order of 0.1% of the final answer and can therefore be neglected in the present calculations.

Expressions (5.8), (5.9) and (5.10) correspond to the static limit when the energy of the thermal photon is zero. To take into account the distribution (5.1) one needs to make the following substitutions in terms (5.8) and (5.9):

$$\frac{\langle mp_j||r||as\rangle}{\Delta\epsilon_{sp}} \to \frac{1}{2}\left[\frac{\langle mp_j||r||as\rangle}{\Delta\epsilon_{sp}+\omega} + \frac{\langle mp_j||r||as\rangle}{\Delta\epsilon_{sp}-\omega}\right], \tag{5.11}$$

and in term (5.10)

$$\frac{1}{\Delta\epsilon_{sp}^2} \to \frac{1}{2}\left[\frac{1}{(\Delta\epsilon_{sp}+\omega)^2} + \frac{1}{(\Delta\epsilon_{sp}-\omega)^2}\right], \tag{5.12}$$

where ω is the frequency of thermal photon. Integrating the resulting expression with (5.1) and keeping only terms up to ω^2 (since $\omega \ll \Delta\epsilon_{sp}$) leads to an expression of the form (5.3) in which the first term is given by (5.8), (5.9) and (5.10) and the parameter ϵ in the second term is given by

$$\epsilon = \frac{A}{k}\left[\sum_i \frac{k_i^{(1)}}{\Delta\epsilon_{spi}^2} + \sum_i \frac{k_i^{(2)}}{\Delta\epsilon_{spi}^2} + 3\sum_i \frac{k_i^{(3)}}{\Delta\epsilon_{spi}^2}\right]. \tag{5.13}$$

Here index i replaces all indexes of summation in (5.8), (5.9) and (5.10), $k_i^{(1)}$ corresponds to terms in (5.8), $k_i^{(2)}$ corresponds to (5.9), $k_i^{(3)}$ corresponds to (5.10) and $k = k^{(1)} + k^{(2)} + k^{(3)}$. $\Delta\epsilon_{spi}$ is the energy of the $s - p$ transition number i. If energies $\Delta\epsilon_{spi}$ are in atomic units then $A = 1.697 \times 10^{-5}$ (the atomic unit of energy is 27.211 eV = 315773K). Lowest $s - p$ transitions (e.g., $6s - 6p_{1/2}$ and $6s - 6p_{3/2}$) strongly dominate in the summation (5.13).

5.3 Calculations

In order to calculate the frequency shift of the hfs transitions due to the electric field one needs to have a complete set of states and to have the energies, electric dipole transition amplitudes and hyperfine structure matrix elements corresponding to these states. It is possible to consider summation over the physical states and use experimental data to perform the calculations. The lowest valence states for which experimental data is usually available dominate the summation. Off-diagonal hfs matrix elements can be obtained to a high accuracy as the square root of the product of corresponding hfs constants: $A_{m,n} = \sqrt{A_m A_n}$ (see, e.g. [36]). However, the accuracy of this approach is limited by the need to include the *tail* contribution from highly excited states including states in the continuum. This contribution can be very significant and its calculation is not easier than the calculation of the whole sum. Also, for atoms like Yb^+ and Hg^+ available experimental data is insufficient to follow this path.

Therefore, we use an *ab initio* approach in which high accuracy is achieved by the inclusion of all important many-body and relativistic effects. We make only one exception toward the semiempirical approach. The frequency shift is dominated by the term (5.10) which is proportional to the hfs in the ground state. These hfs constants are known to very high accuracy from measurements for all atoms considered in the present work. It is natural to use experimental hfs con-

stants in the dominating term to have more accurate results. Note however that the difference with complete *ab initio* calculations is small. It is also instructive to perform calculations of the hfs and atomic polarizabilities to demonstrate the accuracy of the method.

Calculations start from the relativistic Hartree-Fock (RHF) method in the V^{N-1} approximation. This means that the initial RHF procedure is done for a closed-shell atomic core with the valence electron removed. After that, states of the external electron are calculated in the field of the frozen core. Correlations are included by means of the correlation potential method [94]. We use two different approximations for the correlation potential, $\hat{\Sigma}$. First, we calculate it in the lowest, second-order of many-body perturbation theory (MBPT). We use the notation $\hat{\Sigma}^{(2)}$ for the corresponding correlation potential. Then we also include into $\hat{\Sigma}$ two classes of the higher-order terms: screening of the Coulomb interaction and hole-particle interaction (see, e.g. [95] for details). These two effects are included in all orders of MBPT and the corresponding correlation potential is named $\hat{\Sigma}^{(\infty)}$.

To calculate $\hat{\Sigma}^{(2)}$ we need a complete set of single-electron orbitals. We use the B-spline technique [53, 55] to construct the basis. The orbitals are built as linear combinations of 50 B-splines in a cavity of radius $40a_B$. The coefficients are chosen from the condition that the orbitals are eigenstates of the RHF Hamiltonian $\hat{H}_0$ of the closed-shell core. The $\hat{\Sigma}^{(\infty)}$ operator is calculated using a technique that combines solving equations for the Green functions (for the direct diagram) with the summation over the complete set of states (exchange diagram).

The correlation potential $\hat{\Sigma}$ is then used to build a new set of single-electron states, the so-called Brueckner orbitals. This set is to be used in the summation in equations (5.8), (5.9) and (5.10). Here again we use the B-spline technique to build the basis. The procedure is very similar to the construction of the RHF B-spline basis. The only difference is that new orbitals are now the eigenstates

Table 5.1: Rescaling parameters for the $\hat{\Sigma}$ operator which fit energies of the lowest s and p states of Rb, Cs, Ba,$^+$, Yb$^+$ and Hg$^+$.

Atom	$\hat{\Sigma}$	$s_{1/2}$	$p_{1/2}$	$p_{3/2}$
Rb	$\hat{\Sigma}^{(2)}$	0.868	0.903	0.906
Rb	$\hat{\Sigma}^{(\infty)}$	1.008	0.974	0.976
Cs	$\hat{\Sigma}^{(2)}$	0.802	0.848	0.852
Cs	$\hat{\Sigma}^{(\infty)}$	0.985	0.95	0.95
Ba$^+$	$\hat{\Sigma}^{(2)}$	0.782	0.830	0.833
Ba$^+$	$\hat{\Sigma}^{(\infty)}$	0.988	0.963	0.967
Yb$^+$	$\hat{\Sigma}^{(2)}$	0.866	1.09	1.185
Hg$^+$	$\hat{\Sigma}^{(2)}$	0.805	0.890	0.926

of the $\hat{H}_0 + \hat{\Sigma}$ Hamiltonian, where $\hat{\Sigma}$ is either $\hat{\Sigma}^{(2)}$ or $\hat{\Sigma}^{(\infty)}$.

We use the all-order correlation potential $\hat{\Sigma}^{(\infty)}$ for Rb, Cs and Ba$^+$. It has been demonstrated in a number of works (see, e.g. [95–97]) that inclusion of the screening of the Coulomb interaction and the hole-particle interaction leads to very accurate results for alkali atoms. However, for other atoms with one external electron above closed shells these two higher-order effects are not dominating and their inclusion generally does not improve the results. Therefore, for the Yb$^+$ and Hg$^+$ ions we use only the second-order correlation potential $\hat{\Sigma}^{(2)}$.

Brueckner orbitals which correspond to the lowest valence states are good approximations of the real physical states. Their quality can be checked by comparing experimental and theoretical energies. Moreover, their quality can be further improved by rescaling the correlation potential $\hat{\Sigma}$ to fit experimental energies exactly. We do this by replacing the $\hat{H}_0+\hat{\Sigma}$ with the $\hat{H}_0+\lambda\hat{\Sigma}$ Hamiltonian in which the rescaling parameter λ is chosen for each partial wave to fit the energy of the first valence state. The values of λ are presented in Table 5.1. Note that all values are very close to unity. This means that even without rescaling the accuracy is very good and only a small adjustment to the value of $\hat{\Sigma}$ is needed. Note also that since the rescaling procedure effects both energies and

wave functions, it usually leads to improved values of the matrix elements of external fields. In fact, this is a semiempirical method to include omitted higher-order correlation corrections.

Matrix elements of the hfs and electric dipole operators are found by means of the time-dependent Hartree-Fock (TDHF) method [94, 98]. This method is equivalent to the well-known random-phase approximation (RPA). In the TDHF method, single-electron wave functions are presented in the form $\psi = \psi_0 + \delta\psi$, where ψ_0 is unperturbed wave function. It is an eigenstate of the RHF Hamiltonian $\hat{H}_0$: $(\hat{H}_0 - \epsilon_0)\psi_0 = 0$. $\delta\psi$ is the correction due to external field. It can be found by solving the TDHF equation

$$(\hat{H}_0 - \epsilon_0)\delta\psi = -\delta\epsilon\psi_0 - \hat{F}\psi_0 - \delta\hat{V}^{N-1}\psi_0, \tag{5.14}$$

where $\delta\epsilon$ is the correction to the energy due to external field ($\delta\epsilon \equiv 0$ for the electric dipole operator), $\hat{F}$ is the operator of the external field ($\hat{H}_{hfs}$ or $e\boldsymbol{E}\cdot\boldsymbol{r}$), and $\delta\hat{V}^{N-1}$ is the correction to the self-consistent potential of the core due to external field. The TDHF equations are solved self-consistently for all states in the core. Then matrix elements between any (core or valence) states n and m are given by

$$\langle\psi_n|\hat{F} + \delta\hat{V}^{N-1}|\psi_m\rangle. \tag{5.15}$$

The best results are achieved when ψ_n and ψ_m are Brueckner orbitals calculated with rescaled correlation potential $\hat{\Sigma}$.

We use equation (5.15) for all hfs and electric dipole matrix elements in (5.8), (5.9), and (5.10) except for the ground state hfs matrix element in (5.10) where we use experimental data.

To check the accuracy of the calculations we perform calculations of the hfs in the ground state and of the static scalar polarizabilities of the atoms. Polarizabilities are given by the expression

$$\alpha_0(a) = \frac{2}{3}\sum_m \frac{|\langle a||r||m\rangle|^2}{(\epsilon_a - \epsilon_m)} \tag{5.16}$$

which is very similar to the term (5.10) for the frequency shift. The most important difference is that the energy denominator is squared in term (5.10) but not in (5.16). This means better convergence with respect to the summation over complete set of states for term (5.10) than for (5.16). Therefore, if good accuracy is achieved for polarizabilities, even better accuracy should be expected for the term (5.10) (see also Ref. [91]).

However, the behavior of the other two terms, (5.8) and (5.9), is very different and the calculation of polarizabilities tells us little about accuracy for these terms. Therefore, we also perform detailed calculations of the hfs constants of the ground state. Inclusion of core polarization (second term in (5.15)) involves summation over the complete set of states similar to what is needed for term (5.8). Comparing experimental and theoretical hfs is a good test of the accuracy of this term.

The results for polarizabilities, calculated in different approximations, are presented in Table 5.2. Pure *ab initio* results obtained with $\hat{\Sigma}^{(\infty)}$ and results obtained with rescaled correlation potential operators $\hat{\Sigma}^{(2)}$ and $\hat{\Sigma}^{(\infty)}$ are very close to each other and to other calculations and measurements.

In addition to term (5.15), we also include two smaller contributions to the hfs: structure radiation and the correction due to the change of the normalization of the wave function. The structure radiation term can be presented in the form

$$A_{str} = \langle\psi_n|\delta\hat{\Sigma}|\psi_n\rangle, \tag{5.17}$$

where $\delta\hat{\Sigma}$ is the correction to the correlation potential due to external hfs field. The normalization term is

$$A_{norm} = -A_n\langle\psi_n|\frac{\partial\hat{\Sigma}}{\partial\epsilon}|\psi_n\rangle, \tag{5.18}$$

where A_n is given by (5.15) with $m = n$.

The results for hfs are presented in Table 5.3. Here column marked as 'Brueck' corresponds to the $\langle\psi_n|\hat{F}|\psi_n\rangle$ matrix element. The column marked as RPA is the

Table 5.2: Static polarizabilities α_0 of Rb, Cs, Ba,$^+$, Yb$^+$ and Hg$^+$ in different approximations (a_0^3).

Atom		$\hat{\Sigma}$	α_v[a]	α_c[b]	Total	Other works
^{87}Rb	$5s$	$\hat{\Sigma}^{(2)}$[c]	292.7	9.1	301.8	329(23)[f]
		$\lambda\hat{\Sigma}^{(2)}$[d]	309.7	9.1	318.8	293(6)[g]
		$\hat{\Sigma}^{(\infty)}$[e]	312.4	9.1	321.5	318.6(6)[h]
		$\lambda\hat{\Sigma}^{(\infty)}$[d]	310.5	9.2	319.7	318.5(6)[i]
^{133}Cs	$6s$	$\hat{\Sigma}^{(2)}$[c]	343.8	15.3	359.1	401.0(6)[j]
		$\lambda\hat{\Sigma}^{(2)}$[d]	383.5	15.4	399.0	401.5[h]
		$\hat{\Sigma}^{(\infty)}$[e]	384.0	15.5	399.5	400.4[k]
		$\lambda\hat{\Sigma}^{(\infty)}$[d]	384.4	15.5	399.9	400.6(1.0)[l]
^{137}Ba$^+$	$6s$	$\hat{\Sigma}^{(2)}$[c]	104.1	9.8	113.8	
		$\lambda\hat{\Sigma}^{(2)}$[d]	112.5	9.9	122.4	
		$\hat{\Sigma}^{(\infty)}$[e]	112.8	9.9	122.7	
		$\lambda\hat{\Sigma}^{(\infty)}$[d]	112.7	9.9	122.7	
^{171}Yb$^+$	$6s$	$\hat{\Sigma}^{(2)}$[c]	50.9	6.2	57.1	
		$\lambda\hat{\Sigma}^{(2)}$[d]	55.4	6.1	61.5	
^{199}Hg$^+$	$6s$	$\hat{\Sigma}^{(2)}$[c]	10.5	7.7	18.2	
		$\lambda\hat{\Sigma}^{(2)}$[d]	11.4	7.6	19.0	

[a] Polarizability due to valence electron.
[b] Polarizability of the core.
[c] $\hat{\Sigma}^{(2)}$ is the second-order correlation potential.
[d] Rescaled $\hat{\Sigma}$. See Table 5.1 for the values of rescaling factors λ.
[e] $\hat{\Sigma}^{(\infty)}$ is the all-order correlation potential.
[f] Measurements, Ref. [99].
[g] Measurements, Ref. [100].
[h] Calculations, Ref. [101].
[i] Calculations, Ref. [102].
[j] Measurements, Ref. [103].
[k] Calculations, Ref. [104].
[l] Calculations, Ref. [91].

Table 5.3: Contributions to the hyperfine structure of the ground state of Rb, Cs, Ba,$^+$, Yb$^+$ and Hg$^+$ (MHz); comparison with experiment.

Atom		Brueck	RPA	Str	Norm	Total	Exp
^{87}Rb	$5s$	2888	559	-27	-33	3386	3417[a]
^{133}Cs	$6s$	1957	355	-10	-31	2278	2298[a]
^{137}Ba$^+$	$6s$	3509	601	-21	-73	4016	4019[b]
^{171}Yb$^+$	$6s$	11720	1540	-248	-247	12764	12645(2)[c]
^{199}Hg$^+$	$6s$	38490	3873	288	-1483	41169	40507[d]

[a] Reference [105].
[b] References [106] and [107].
[c] Reference [108].
[d] Reference [109].

core polarization correction given by $\langle\psi_n|\delta\hat{V}^{N-1}|\psi_n\rangle$, the notation 'Str' stands for structure radiation given by (5.17), and 'Norm' is the renormalization contribution given by (5.18). In all cases ψ_n is the Bruckner orbital corresponding to the ground state of the atom or ion, calculated with the rescaled correlation potential $\hat{\Sigma}$. All-order $\hat{\Sigma}^{(\infty)}$ is used for Rb, Cs and Ba$^+$. Second-order $\hat{\Sigma}^{(2)}$ is used for Yb$^+$ and Hg$^+$. Comparing the final theoretical results with experiment shows that the theoretical accuracy is within 1% for all atoms except Hg$^+$ where it is 1.6%. If the structure radiation and normalization are neglected, accuracy for Rb and Cs remains within 1%, accuracy for Ba$^+$ becomes about 2% and accuracy for Yb$^+$ and Hg$^+$ becomes close to 5%.

5.4 Results and discussion

Table 5.4 presents contributions of terms (5.8), (5.9) and (5.10) into the total frequency shift of the hfs transitions for the ground states of ^{87}Rb, ^{133}Cs, ^{137}Ba$^+$, ^{171}Yb$^+$ and ^{199}Hg$^+$ calculated in different approximations. Term (5.10) dominates in all cases, while term (5.9) is small but still important at least for Rb, Cs and Ba$^+$. Results obtained with $\hat{\Sigma}^{(2)}$ and $\hat{\Sigma}^{(\infty)}$ differ significantly (up to 14% for

Cs). However, after rescaling, the results for both $\hat{\Sigma}^{(2)}$ and $\hat{\Sigma}^{(\infty)}$ come within a fraction of a per cent of each other. Naturally, rescaling has a larger effect on results obtained with $\hat{\Sigma}^{(2)}$. This means that the rescaling really imitates the effect of higher-order correlations and should lead to more accurate results. Comparing the results obtained with $\hat{\Sigma}^{(\infty)}$, rescaled $\hat{\Sigma}^{(\infty)}$ and rescaled $\hat{\Sigma}^{(2)}$ gives a reasonable estimation of the accuracy of calculations. If we also combine this with the calculation of the hfs discussed above we can safely assume that the accuracy of the calculations for Rb, Cs and Ba^+ is on the level of 1%. Note that the frequency shift due to blackbody radiation can be a little larger ($\sim 1\%$) due to the effect of frequency distribution at finite temperature (this effect is incorporated into our result using the ϵ term in Eq. (5.3), and so should not be considered an additional uncertainty).

For Yb^+ and Hg^+ we only have results with rescaled $\hat{\Sigma}^{(2)}$ and not rescaled $\hat{\Sigma}^{(\infty)}$. They differ by about 11%. However, there are strong reasons to believe that the results obtained with rescaling are more accurate. This is supported by calculations for Rb, Cs and Ba^+ as well as our experience with rescaling used in many earlier works. Therefore, the calculation of the hfs discussed above gives a more realistic estimation of the accuracy for Yb^+ and Hg^+ which is about 5%.

Table 5.4 presents values of k (see formula (5.4)). To obtain the frequency shift at finite temperature one needs to convert k into β using formula (5.5) and substitute β into equation (5.3). For accurate results one also needs to know the values of ϵ. We calculate them using formula (5.13) in a very similar way to how we calculate parameters k. Our final values of k, β and ϵ are presented in Table 5.5. Parameter ϵ for Cs was estimated in the single-resonance approximation in [81] and found to be 0.014. This value is in good agreement with our accurate calculations.

The frequency shifts of some alkali metal atoms have been calculated and measured previously. We present previous results for the atoms and ions for

Table 5.4: Contribution of terms (5.8), (5.9), and (5.10) to the frequencies of the hyperfine transitions in the ground state of Rb, Cs, Ba,$^+$, Yb$^+$ and Hg$^+$ ($\delta\nu_0/E^2 \times 10^{-10}$ Hz/(V/m)^2) in different approximations.

Atom		$\hat{\Sigma}$	(5.8)	(5.9)	(5.10)	Total
^{87}Rb	$5s$	$\hat{\Sigma}^{(2)a}$	-0.5457	0.0147	-0.6692	-1.2003
		$\lambda\hat{\Sigma}^{(2)b}$	-0.5668	0.0154	-0.6894	-1.2409
		$\hat{\Sigma}^{(\infty)c}$	-0.5640	0.0156	-0.7034	-1.2518
		$\lambda\hat{\Sigma}^{(\infty)b}$	-0.5620	0.0154	-0.6972	-1.2437
^{133}Cs	$6s$	$\hat{\Sigma}^{(2)a}$	-0.9419	0.0210	-1.0722	-1.9931
		$\lambda\hat{\Sigma}^{(2)b}$	-1.0239	0.0229	-1.2688	-2.2697
		$\hat{\Sigma}^{(\infty)c}$	-1.0148	0.0232	-1.2706	-2.2622
		$\lambda\hat{\Sigma}^{(\infty)b}$	-1.0167	0.0230	-1.2695	-2.2632
^{137}Ba$^+$	$6s$	$\hat{\Sigma}^{(2)a}$	-0.1027	0.0034	-0.1568	-0.2561
		$\lambda\hat{\Sigma}^{(2)b}$	-0.1095	0.0036	-0.1768	-0.2827
		$\hat{\Sigma}^{(\infty)c}$	-0.1104	0.0037	-0.1778	-0.2845
		$\lambda\hat{\Sigma}^{(\infty)b}$	-0.1104	0.0037	-0.1773	-0.2841
^{171}Yb$^+$	$6s$	$\hat{\Sigma}^{(2)a}$	-0.0672	0.0009	-0.0866	-0.1529
		$\lambda\hat{\Sigma}^{(2)b}$	-0.0714	0.0011	-0.1003	-0.1706
^{199}Hg$^+$	$6s$	$\hat{\Sigma}^{(2)a}$	-0.0242	0.0000	-0.0296	-0.0538
		$\lambda\hat{\Sigma}^{(2)b}$	-0.0263	0.0000	-0.0335	-0.0598

[a] $\hat{\Sigma}^{(2)}$ is the second-order correlation potential.
[b] Rescaled $\hat{\Sigma}$. See Table 5.1 for the values of rescaling factors λ.
[c] $\hat{\Sigma}^{(\infty)}$ is the all-order correlation potential.

Table 5.5: Final results for the parameters k (10^{-10} Hz/(V/m)^2), β (10^{-14}) and ϵ of the black-body radiation frequency shift for Rb, Cs, Ba,$^+$, Yb$^+$ and Hg$^+$.

Atom		k	β	ϵ
^{87}Rb	$5s$	-1.24(1)	-1.26(1)	0.011
^{133}Cs	$6s$	-2.26(2)	-1.70(2)	0.013
^{137}Ba$^+$	$6s$	-0.284(3)	-0.245(2)	0.004
^{171}Yb$^+$	$6s$	-0.171(9)	-0.094(5)	0.002
^{199}Hg$^+$	$6s$	-0.060(3)	-0.0102(5)	0.0005

which we perform calculations in Table 5.6 together with our final results.

There is some disagreement for cesium. Our result is in good agreement with early measurements [82, 83, 85] and *ab initio* calculations [89, 90] while recent measurements [86, 87] and semiempirical calculations [88, 91, 92] give the value which is about 10% smaller. Less accurate measurements of Bauch and Schröder [84] cover both cases. We cannot comment on disagreement between experimental results. However, the source of disagreement between theoretical results seems to be clear. It comes from the contribution of the continuum spectrum to the summation over the complete set of states in term (5.8). This term has off-diagonal hfs matrix elements between the ground state and excited states. Since the hfs interaction is localized over short distances ($\sim a_0/Z$) it emphasizes the contribution of states with high energies including states in the continuum (since $\Delta p \Delta x \geq \hbar$, a small area of localization (Δx) allows high momentum (p) and thus high energy). In our calculations the contribution of states above $7p$ into term (5.8) is $-0.35 \times 10^{-1}\mathrm{Hz}/(\mathrm{V/m})^2$ which is 15% of the total answer.

In contrast, states above $7p$ contribute only about 0.05% of the total value of term (5.10). This is because the summation goes over the matrix elements of the electric dipole operator which is large on large distances and thus suppresses the contribution of high-energy states. It is not surprising therefore that a semiempirical consideration, involving only discrete spectrum states, gives very good results for the atomic polarizabilities (see, e.g. [91]). However, let us stress once more that the calculation of polarizabilities checks only term (5.10) and tells us very little about the accuracy of the other two terms, (5.8) and (5.9).

The contribution of the states above $7p$ is even more important for term (5.9). Their contribution is about 30% of the total value of this term. However, the term itself is small and its accurate treatment is less important.

In *ab initio* calculations by Lee *et al* [89] summation over complete set of states is reduced to solving a radial equation (equations of this type are often

called Sternheimer equation after one of the authors of this work). This approach does include the contribution of the continuum spectrum and the result is in very good agreement with ours (see Table 5.6).

In other *ab initio* calculations by Pal'chikov *et al* [90] summation is done via Green functions. This corresponds to summation over the complete set of states and does include the continuum spectrum. Again, the result is in very good agreement with other *ab initio* calculations ([89] and the present work).

Recent calculations by Beloy *et al* [93] applied a mixed approach, with extensive use of experimental data for lower cesium states and *ab initio* summation over higher states including the continuum. The result is in good agreement with fully *ab initio* calculations.

In contrast, analysis performed in [88, 91, 92] is limited to discrete spectrum. Adding $-0.34 \times 10^{-1}\mathrm{Hz}/(\mathrm{V/m})^2$ (which is total *tail* contribution from all three terms (5.8), (5.9) and (5.10) found in our calculation) to the results of Feitchner *et al* [88] and Micalizio *et al* [91] brings them to excellent agreement with *ab initio* calculations. The same modification of the result by Ulzega *et al* [92] makes it a little bit too large but still closer to other results than without the *tail* contribution.

5.5 Conclusion

We performed calculations of the frequency shift of the ground state hyperfine transition for several atoms and ions caused by a static electric field which can be used to evaluate the effect of blackbody radiation on the frequency of the microwave atomic clock transitions. The size of this shift is comparable to the current error in the measurements of the energy shift caused by variation of α and so needs to be taken into account in laboratory measurements placing limits upon α variation.

Table 5.6: Electrostatic frequency shifts for the hyperfine transitions of Rb, Cs, Ba,$^+$, Yb$^+$ and Hg$^+$ ($\delta\nu_0/E^2 \times 10^{-10}$ Hz/(V/m)^2) ; comparison with other calculations and measurements.

Atom		This work	Other calculations	Ref	Measurements	Ref
^{87}Rb	$5s$	-1.24(1)	-1.2094	[89]	-1.23(3)	[83]
^{133}Cs	$6s$	-2.26(2)	-1.9(2)	[88]	-2.29(7)	[82]
			-2.2302	[89]	-2.25(5)	[83]
			-2.28	[90]	-2.17(26)	[84]
			-1.97(9)	[91]	-2.271(4)	[85]
			-2.06(1)	[92]	-1.89(12)	[86]
			-2.268(8)	[93]	-2.03(4)	[87]
^{137}Ba$^+$	$6s$	-0.284(3)	-0.27	[81]		
^{171}Yb$^+$	$6s$	-0.171(9)				
^{199}Hg$^+$	$6s$	-0.060(3)	-0.058	[81]		

Detailed analysis of the calculations for cesium reveal the source of disagreement between different theoretical approaches. This seems to be the contribution of the continuum spectrum into summation over complete set of states which was neglected in semiempirical calculations. Restoring the *tail* contribution in works where it was neglected brings all theoretical results into good agreement with each other. This correction needs to be applied to measurements made of the hyperfine transition in cesium in order to accurately measure the length of a second.

Chapter 6

Conclusion

This thesis has considered the theoretical calculations that are needed to interpret the results of atomic clock experiments, in order to place limits on the variation of the fine structure constant, α. This is a particularly interesting field of research at the moment because of indications from quasar spectra that α may have been smaller in the past [13].

We have considered how the energy levels in two valence electron atoms and ions will be affected by a change in the value of α. Our calculations of this effect can be used in conjunction with measurements of the change in transition frequencies over time to place tight constraints on α variation.

This thesis has also considered several situations in which a change in the transition frequency over time is greatly enhanced with respect to a change in α. In particular we have considered using atoms with close, narrow levels that will move relative to each other if α is varying. Using a scheme such as this is advantageous for obtaining tight constraints on α variation since less precise experimental results can give competitive constraints on α variation.

We have shown that if the Dirac Hamiltonian is actually perturbed by a dynamically varying α in the manner suggested by Bekenstein [68] then the analysis

used by the quasar groups and also used to interpret atomic clock experiments is still valid.

Finally we have considered how blackbody radiation effects the hyperfine energy levels in some atoms. Blackbody radiation causes the energy levels to shift, and the effect can be of the same order of magnitude as a change in α and so needs to be accounted for. We performed the calculation for the hyperfine levels in cesium that are used as a frequency standard to define the second and showed why there was disagreement among previous results. We also calculated the shift for other atoms and ions. Experiments to constrain α variation are planned for the $^{171}Yb^{+}$ ion [110] and experiments have already been conducted with the $^{199}Hg^{+}$ ion and ^{87}Rb for example. It would not be hard for us to calculate the blackbody shift for many other atoms and ions, of interest for experiments, now that we have shown that our method works.

Appendix A

Table of calculated q coefficients

This is a list of many of the q coefficients that have been accurately calculated by our group. This list may be helpful to an experimentalist planning an experiment to measure α variation.

Table A.1: Experimental energies and calculated q coefficients for transitions from the ground state to the state shown.

Atom/Ion	Z	State		Wavelength, Å	q (cm^{-1})	Reference
				Experiment		
Al II	13	$3s3p$	$^3P_0$	2674.30	146	[1]
		$3s3p$	$^3P_1$	2669.95	211	[1]
		$3s3p$	$^3P_2$	2661.15	343	[1]
		$3s3p$	$^1P_1$	1670.79	278	[1]
Ca I	20	$4s4p$	$^3P_0$	6597.22	125	[1]
		$4s4p$	$^3P_1$	6574.60	180	[1]
		$4s4p$	$^3P_2$	6529.15	294	[1]
		$4s4p$	$^1P_1$	4227.92	250	[1]

Sr I	38	$5s5p$	$^3P_0$	6984.45	443	[1]
		$5s5p$	$^3P_1$	6894.48	642	[1]
		$5s5p$	$^3P_2$	6712.06	1084	[1]
		$5s5p$	$^1P_1$	4608.62	924	[1]
Sr II	38	$4d$	$^2D_{3/2}$	6870.07	2828	[34]
		$4d$	$^2D_{5/2}$	6740.25	3172	[34]
In II	49	$5s5p$	$^3P_0$	2365.46	3787	[1]
		$5s5p$	$^3P_1$	2306.86	4860	[1]
		$5s5p$	$^3P_2$	2182.12	7767	[1]
		$5s5p$	$^1P_1$	1586.45	6467	[1]
Ba II	56	$5d$	$^2D_{3/2}$	20644.74	5844	[111]
		$5d$	$^2D_{5/2}$	17621.70	5976	[111]
Dy I	66	$4f^{10}5d6s$	$^3[10]_{10}$	5051.03	6008	[59]
		$4f^95d^26s$	$^9K_{10}$	5051.03	-23708	[59]
Yb I	70	$6s6p$	$^3P_0$	5784.21	2714	[1]
		$6s6p$	$^3P_1$	5558.02	3527	[1]
		$6s6p$	$^3P_2$	5073.47	5883	[1]
		$6s6p$	$^1P_1$	3989.11	4951	[1]
Yb II	70	$4f^{14}5d$	$^2D_{3/2}$	4355.25	10118	[59]
		$4f^{14}5d$	$^2D_{5/2}$	4109.70	10397	[59]
		$4f^{13}6s^2$	$^2F_{7/2}$	4668.81	-56737	[59]
Yb III	70	$4f^{13}5d$	$^3P_0$	2208.63	-27800	[59]
Hg I	80	$6s6p$	$^3P_0$	2656.39	15299	[1]
		$6s6p$	$^3P_1$	2537.28	17584	[1]
		$6s6p$	$^3P_2$	2270.51	24908	[1]
		$6s6p$	$^1P_1$	1849.50	22789	[1]

Hg II	80	$5d^9 6s^2$	$^2D_{5/2}$	2815.79	-56671	[34]
		$5d^9 6s^2$	$^2D_{3/2}$	1978.16	-44003	[34]
Tl II	81	$6s6p$	$^3P_0$	2022.20	16267	[1]
		$6s6p$	$^3P_1$	1872.90	18845	[1]
		$6s6p$	$^3P_2$	1620.09	33268	[1]
		$6s6p$	$^1P_1$	1322.75	29418	[1]
Ra II	88	$6d$	$^2D_{3/2}$	8275.15	18785	[111]
		$6d$	$^2D_{5/2}$	7276.37	17941	[111]

Appendix B

Acknowledgement of the Atomic Computer Codes

The atomic computer codes used in this thesis have been adapted from a set initially written by V. A. Dzuba, V. V. Flambaum and O. P. Sushkov. The codes begin by generating an approximation of the wavefunction of the core by using the relativistic Hartree-Fock method [112]. The wavefunctions of the valence electrons are then calculate in the field of the frozen core [112]. V. A. Dzuba, V. V. Flambaum and M.G. Kozlov updated the code to using many-body perturbation theory for the interaction between the valence electrons and the core and the configuration interaction to account for interaction between valence electrons [51]. These codes have been improved by using B-splines to form a more complete basis set. This modification was made by V. A. Dzuba based on work he has done with W. R. Johnson [52].

Specific adaptions to these codes have been made for the work presented in chapters 2 and 5. In each of these cases the changes made to the code have been discussed.

Bibliography

[1] E. J. Angstmann, V. A. Dzuba, and V. V. Flambaum, Phys. Rev. A **70**, 014102 (2004).

[2] E. J. Angstmann, V. V. Flambaum, and S. G. Karshenboim, Phys. Rev. A **70**, 044104 (2004).

[3] E. J. Angstmann, V. A. Dzuba, V. V. Flambaum, A. Y. Nevsky, and S. G. Karshemboim, J. Phys. B: At. Mol. Opt. Phys. **39**, 1 (2006).

[4] E. J. Angstmann, V. A. Dzuba, and V. V. Flambaum, Phys. Rev. Lett. **97**, 040802 (2006).

[5] E. J. Angstmann, V. A. Dzuba, and V. V. Flambaum, Phys. Rev. A **74**, 023405 (2006).

[6] E. J. Angstmann, T. H. Dinh, and V. V. Flambaum, Phys. Rev. A **72**, 052105 (2005).

[7] J. P. Uzan, Rev. Mod. Phys. **75**, 403 (2003).

[8] P. Langacker, G. Sergrè, and M. Strassler, Phys. Lett. B **528**, 121 (2002).

[9] X. Calmet and H. Fritzsch, Eur. Phys. J. C **24**, 639 (2002).

[10] V. V. Flambaum and E. V. Shuryak, Phys. Rev. D **65**, 103503 (2002).

[11] V. F. Dmitriev and V. V. Flambaum, Phys. Rev. D **67**, 063513 (2003).

[12] C. Chin and V. V. Flambaum, Phys. Rev. Lett. **96**, 230801 (2006).

[13] J. K. Webb, V. V. Flambaum, C. W. Churchill, M. J. Drinkwater, and J. D. Barrow, Phys. Rev. Lett. **82**, 884 (1999).

[14] H. Sandvik, J. Barrow, and J. Magueijo, Phys. Rev. Lett. **88**, 031302 (2002).

[15] M. T. Murphy, J. K. Webb, and V. V. Flambaum, Mon. Not. R. Astron. Soc. **345**, 609 (2003).

[16] R. Quast, D. Reimers, and S. A. Levshakov, Astron. Astrophys. **415**, L7 (2004).

[17] R. Srianand, H. Chand, P. Petitjean, and B. Aracil, Phys. Rev. Lett. **92**, 121302 (2004).

[18] M. T. Murphy, J. K. Webb, and V. V. Flambaum, arXiv:astro-ph/0612407 (2006).

[19] A. I. Shlyakhter, Nature **264**, 340 (1976).

[20] T. Damour and F. Dyson, Nucl. Phys. B **480**, 596 (1994).

[21] Y. Fujii, A. Iwamoto, T. Fukahori, T. Ohnuki, M. Nakagawa, H. Hidaka, Y. Oura, and P. Moller, Nucl. Phys. B **573**, 377 (2000).

[22] S. K. Lamoreaux and J. R. Torgerson, Phys. Rev. D **69**, 121701(R) (2004).

[23] K. A. Olive, M. Pospelov, Y. Z. Qian, G. Manhès, E. Vangioni-Flam, A. Coc, and M. Cassé, Phys. Rev. D **69**, 027701 (2004).

[24] V. V. Flambaum and E. V. Shuryak, Phys. Rev. D **67**, 083507 (2003).

[25] H. Marion, F. P. D. Santos, M. Abgrall, S. Zhang, Y. Sortais, S. Bize, I. Maksimovic, J. G. D. Calonico, C. Mandache, P. Lemonde, G. Santarelli, P. Laurent, A. Clairon, and C. Salomon, Phys. Rev. Lett. **90**, 150801 (2003).

[26] E. Peik, B. Lipphardt, H. Schnatz, T. Schneider, C. Tamm, and S. G. Karshemboim, Phys. Rev. Lett. **93**, 170801 (2004).

[27] E. Peik, B. Lipphardt, H. Schnatz, C. Tamm, S. Weyers, and R. Wynands, in H. Kleinert, R. T. Jantzen, and R. Ruffini (editors), *Proceedings of the 11th Marcel Grossman Meeting on General Relativity* (World Scientific, 2007), `arXiv:phys/0611088`.

[28] T. Udem, S. A. Diddams, K. R. Vogel, C. W. Oates, E. A. Curtis, W. D. Lee, W. M. Itano, R. E. Drullinger, J. C. Bergquist, and L. Hollberg, Phys. Rev. Lett. **86**, 4996 (2001).

[29] S. Bize, S. A. Diddams, U. Tanaka, C. E. Tanner, W. H. Oskay, R. E. Drullinger, T. E. Parker, T. P. Heavner, S. R. Jefferts, J. Hollberg, W. M. Itano, and J. C. Bergquist, Phys. Rev. Lett **90**, 150802 (2003).

[30] W. H. Oskay, S. A. Diddams, E. A. Donley, T. M. Fortier, T. P. Heavner, L. Hollberg, W. M. Itano, S. R. Jefferts, M. J. Delaney, K. Kim, F. Levi, T. E. Parker, and J. C. Bergquist, Phys. Rev. Lett. **97**, 020801 (2006).

[31] S. G. Karshenboim, Can. J. Phys. **78**, 639 (2000).

[32] V. V. Flambaum and A. F. Tedesco, Phys. Rev. C **73**, 055501 (2006).

[33] A. T. Nguyen, D. Budker, S. K. Lamoreaux, and J. R. Torgerson, Phys. Rev. A **69**, 022105 (2004).

[34] V. A. Dzuba, V. V. Flambaum, and J. K. Webb, Phys. Rev. A **59**, 230 (1999).

[35] V. A. Dzuba, V. V. Flambaum, M. G. Kozlov, and M. V. Marchenko, Phys. Rev. A **66**, 022501 (2002).

[36] V. A. Dzuba and V. V. Flambaum, Phys. Rev. A **62**, 052101 (2000).

[37] A. Cingöz, A. Lapierre, A. T. Nguyen, N. Leefer, D. Budker, S. K. Lamoreaux, and J. R. Torgerson, arXiv:physics/0609014 (2006).

[38] M. Fischer, N. Kolachevsky, M. Zimmermann, F. P. D. Santos, P. Lemonde, G. Santarelli, P. Laurent, A. Clairon, C. Salmon, M. Haas, U. D. Jentschura, and C. H. Keitel, Phys. Rev. Lett. **92**, 230802 (2004).

[39] J. D. Prestage, R. Tjoelker, and L. Maleki, Phys. Rev. Lett. **74**, 3511 (1995).

[40] A. Godone, C. Novero, P. Tavella, and K. Rahimullah, Phys. Rev. Lett. **71**, 2364 (1993).

[41] E. J. Angstmann, V. A. Dzuba, and V. V. Flambaum, arXiv:physics/0407141 (2004).

[42] D. J. Wineland*et al.*, (unpublished) .

[43] I. Courtillot, A. Quessada, R. P. Kovacich, A. Brusch, D. Kolker, J. Zondy, G. D. Rovera, and P. Lemonde, Phys. Rev. A **68**, 030501 (2003).

[44] H. Katori, M. Takamoto, V. G. Pal'chikov, and V. D. Ovisiannikov, Phys. Rev. Lett. **91**, 173005 (2003).

[45] M. Takomoto and H. Katori, Phys. Rev. Lett **91**, 223001 (2003).

[46] T. Becker *et al.*, (unpublished) .

[47] W. Nagourney, (unpublished) .

[48] J. von Zanthier *et al.*, Opt. Lett. **25**, 1729 (2000).

[49] S. Bize, private communication .

[50] S. G. Porsev, A. Derevianko, and E. N. Fortson, Phys. Rev. A **69**, 021403 (2004).

[51] V. A. Dzuba, V. V. Flambaum, and M. Kozlov, Phys. Rev. A **54**, 3948 (1996).

[52] V. A. Dzuba and W. R. Johnson, Phys. Rev. A **57**, 2459 (1998).

[53] W. R. Johnson and J. Sapirstein, Phys. Rev. Lett. **57**, 1126 (1986).

[54] W. R. Johnson, M. Idrees, and J. Sapirstein, Phys. Rev. A **35**, 3218 (1987).

[55] W. R. Johnson, S. A. Blundell, and J. Sapirstein, Phys. Rev. A **37**, 307 (1988).

[56] C. E. Moore, *Atomic Energy Levels, Natl. Bur. Stand. (U.S.) Circ. No. 35 Vols. I and II* (U.S. GPO, 1971).

[57] S. G. Porsev, Y. G. Rakhliana, and M. G. Kozlov, J. Phys. B **32**, 1113 (1999).

[58] S. G. Porsev, M. G. Kozlov, Y. G. Rakhlina, and A. Derevianko, Phys. Rev. A **64**, 012508 (2001).

[59] V. A. Dzuba, V. V. Flambaum, and M. V. Marchenko, Phys. Rev. A **68**, 022506 (2003).

[60] V. B. Berestetskii, E. M. Lifshitz, and L. P. Pitaevskii, *Quantum Electrodynamics* (Butterworth-Heinemann, 1982).

[61] A. T. Nguyen, D. Budker, D. DeMille, and M. Zolotorev, Phys. Rev. A **56**, 3453 (1997).

[62] V. A. Dzuba and V. V. Flambaum, Phys. Rev. A **72**, 052514 (2005).

[63] *NIST Atomic Spectral Database Version 3.0.3 Jan 2006 can be obtained from: http://physics.nist.gov/PhysRefData/ASD/index.html.*

[64] D. J. Wineland, J. C. Bergquist, J. J. Bollinger, R. E. Drullingen, and W. M. Itano, in P. Gill (editor), *Proceedings of the 6th Symposium Frequency Standards and Meterology*, 361 (World Scientific, 2002).

[65] P. O. Schmidt, T. Rosenband, C. Langer, W. M. Itano, J. C. Bergquist, and D. J. Wineland, Science **309**, 749 (2005).

[66] V. V. Flambaum, Phys. Rev. Lett. **97**, 092502 (2006).

[67] V. V. Flambaum, Phys. Rev. A **73**, 034101 (2006).

[68] J. D. Bekenstein, astro-ph/0301566 (2003).

[69] V. A. Dzuba, V. V. Flambaum, and J. K. Webb, Phys. Rev. Lett. **82**, 888 (1999).

[70] L. D. Landau and E. M. Lifshitz, *Quantum Mechanics* (Butterworth-Heinemann, 1977).

[71] I. B. Khriplovich, *Parity Nonconservation in Atomic Phenomena* (Gordon and Breach, 1991).

[72] J. C. Slater, Phys. Rev. **34**, 1293 (1929).

[73] J. C. Slater, Phys. Rev. **38**, 1109 (1931).

[74] S. R. Lundeen and F. M. Pipkin, Metrologia **22**, 9 (1986).

[75] E. W. Hayley and F. M. Pipkin, Phys. Rev. Lett. **71**, 1172 (1994).

[76] P. J. Mohr and B. N. Taylor, Rev. Mod. Phys. **72**, 351 (2000).

[77] M. I. Eides, H. Grotch, and V. A. Shelyuto, Phys. Rep. **72**, 63 (2001).

[78] A. Wicht, J. M. Hensley, E. Sarajilic, and S. Chu, in P. Gill (editor), *Proceedings of the 6th Symposium Frequency Standards and Metrology*, 193 (World Scientific, 2002).

[79] T. Kinoshita and M. Nio, Phys. Rev. Lett. **90**, 021803 (2003).

[80] J. K. Webb, M. T. Murphy, V. V. Flambaum, V. A. Dzuba, J. D. Barrow, C. W. Churchill, J. X. Prochaska, and A. M. Wolfe, Phys. Rev. Lett. **87**, 091301 (2001).

[81] W. M. Itano, L. L. Lewis, and D. J. Wineland, Phys. Rev. A **25**, 1233 (1982).

[82] R. D. Haun and J. R. Zacharias, Phys. Rev. **107**, 107 (1957).

[83] J. R. Mowat, Phys. Rev. A **5**, 1059 (1972).

[84] A. Bauch and R. Schröder, Phys. Rev. Lett. **78**, 622 (1997).

[85] E. Simon, P. Laurent, and A. Clairon, Phys. Rev. A **57**, 436 (1998).

[86] F. Levi, D. Calonico, L. Lorini, S. Micalisio, and A. Godone, Phys. Rev. A **70**, 033412 (2004).

[87] A. Godone, D. Calonico, F. Levi, S. Micalzio, and C. Calosso, Phys. Rev. A **71**, 063401 (2005).

[88] J. D. Feitchner, M. E. Hoover, and M. Mitzushima, Phys. Rev. **137**, A702 (1965).

[89] T. Lee, T. P. Das, and R. M. Sternheimer, Phys. Rev. A **11**, 1784 (1975).

[90] V. G. Pal'chikov, Y. S. Domnin, and A. V. Novoselov, J. Opt. B: Quantum Semiclassical Opt. **5**, S131 (2003).

[91] S. Micalizio, A. Godone, D. Calonico, F. Levi, and L. Lorini, Phys. Rev. A **69**, 053401 (2004).

[92] S. Ulzega, A. Hofer, P. Moroshkin, and A. Weis, physics/0604233 (2006).

[93] K. Beloy, U. I. Safronova, and A. Derevianko, Phys. Rev. Lett. **97**, 040801 (2006).

[94] V. A. Dzuba, V. V. Flambaum, P. G. Silverstrov, and O. P. Sushkov, J. Phys. B: At. Mol. Phys **20**, 1399 (1987).

[95] V. A. Dzuba, V. V. Flambaum, and O. P. Sushkov, Phys. Lett. A **141**, 147 (1989).

[96] V. A. Dzuba, V. V. Flambaum, and O. P. Sushkov, Phys. Rev. A **51**, 3454 (1995).

[97] V. A. Dzuba, V. V. Flambaum, and J. S. M. Ginges, Phys. Rev. A **63**, 062101 (2001).

[98] V. A. Dzuba, V. V. Flambaum, and O. P. Sushkov, J. Phys. B: At. Mol. Phys. **17**, 1953 (1984).

[99] R. W. Molof, H. L. Schwartz, T. M. Miller, and B. Bederson, Phys. Rev. A **10**, 1131 (1974).

[100] W. D. Hall and J. C. Zorn, Phys. Rev. A **10**, 1141 (1974).

[101] A. Derevianko, W. R. Johnson, M. S. Safronova, and J. F. Babb, Phys. Rev. Lett. **82**, 3589 (1999).

[102] M. S. Safronova, C. J. Williams, and C. W. Clark, Phys. Rev. A **67**, 040303(R) (2003).

[103] J. M. Amini and H. Gould, Phys. Rev. Lett. **91**, 153001 (2003).

[104] A. Derevianko and S. G. Porsev, Phys. Rev. A **65**, 53403 (2002).

[105] G. H. Fuller and V. W. Cohen, Nucl. Data, Sect. A **5**, 433 (1969).

[106] J. Vetter, M. Stuke, and E. W. Weber, The Euro. Phys. J. A **273**, 129 (1975).

[107] S. Trapp, G. Marx, G. Tommaseo, A. Klaas, A. Drakoudis, G. Revalde, G. Szawiola, and G. Werth, Hyperfine Interactions **127**, 57 (2000).

[108] A. M. Mårtensson-Pendrill, D. S. Gough, and P. Hannaford, Phys. Rev. A **49**, 3351 (1994).

[109] D. J. Berkeland, J. D. Miller, B. C. Young, J. C. Bergquist, W. M. Itano, and D. J. Wineland, Proc. SPIE **3270**, 138 (1998).

[110] B. Warrington, private communication .

[111] V. A. Dzuba and V. V. Flambaum, Phys. Rev. A **61**, 034502 (2000).

[112] V. V. F. V. A. Dzuba and O. P. Sushkov, J. Phys. B: At. Mol. Phys. **16**, 715 (1983).